Meteoritics & Planetary Science 41, Nr 6, 953–976 (2006)
Abstract available online at http://meteoritics.org

Stellar nucleosynthetic contribution of extinct short-lived nuclei in the early solar system and the associated isotopic effects

S. SAHIJPAL* and P. SONI

Department of Physics, Panjab University, Chandigarh, India 160014
*Corresponding author. E-mail: sandeep@pu.ac.in

(Received 12 October 2004; revision accepted 13 February 2006)

Abstract–A wide range of stellar nucleosynthetic sources has been analyzed to derive their contributions of short-lived and stable nuclei to the presolar cloud. This detailed study is required to infer the most plausible source(s) of short-lived nuclei through a critical comparison among the various stellar sources that include AGB stars, novae, supernovae II, Ia, and Wolf-Rayet stars that evolved to supernovae Ib/c. In order to produce the canonical value of $^{26}Al/^{27}Al$ in the early solar system, almost all stellar sources except low-mass AGB stars imply large isotopic anomalies in Ca-Al-rich inclusions (CAIs). This is contrary to the observed isotopic compositions of CAIs. The discrepancy could impose stringent constraints on the formation and thermal evolution of CAIs from different chondrites. Among the various stellar scenarios, the injection of short-lived nuclei into the previously formed solar protoplanetary disc by a massive star of an ad hoc chosen high-injection mass cut is a possible scenario. There is a possibility of the contribution of short-lived nuclides by a 1.5–3 $M_\odot$ AGB star as it implies the smallest shift in stable isotopes. A low-mass AGB star of relatively low metallicity would be even a better source of short-lived nuclei. However, this scenario would require independent gravitational collapse of the presolar cloud coupled with ambipolar diffusion of magnetic flux. Alternatively, numerous scenarios can be postulated that involve distant (≥10 pc) massive stars can contribute ^{60}Fe to the presolar cloud and can trigger its gravitational collapse. These scenarios would require production of ^{26}Al and ^{41}Ca by irradiation in the early solar system. Significant production of ^{26}Al and ^{60}Fe can be explained if massive, rotating Wolf-Rayet stars that evolved to supernovae Ib/c were involved.

INTRODUCTION

The presence of several short-lived nuclei, e.g., $^{7,10}Be$, ^{41}Ca, ^{36}Cl, ^{26}Al, ^{60}Fe, and ^{53}Mn (mean lives, $\tau \leq 5$ Ma) in the early solar system has spurred a vigorous debate on the initial conditions that led to the formation of the solar system (Podosek and Nichols 1997; Meyer and Clayton 2000; Goswami and Vanhalla 2000; McKeegan et al. 2000; Chaussidon et al. 2004). Diverse stellar nucleosynthetic sources (Cameron 1993; MacPherson et al. 1995; Cameron et al. 1995, 1997; Desch and Ouellette 2005; Wasserburg et al. 2006) and irradiation scenarios (Lee et al. 1998; Shu et al. 2001; Leya et al. 2003; Sahijpal and Soni 2004, 2006) have been proposed to explain the presence of these short-lived nuclei in the early solar system. The stellar nucleosynthetic scenario postulates late-stage injection of short-lived nuclei by a "nearby" evolved star into the presolar cloud. The event may or may not have triggered the gravitational collapse of the presolar cloud, leading to the formation of the solar system (Cameron and Truran 1977; Cameron et al. 1995, 1997; Sahijpal et al. 1998). Conversely, other scenarios involve irradiation of dust and gas in the nebula by energetic particles from magnetic flaring events associated with the protosun and/or its circumstellar accretion disc (Feigelson et al. 2002). In contrast to most of the stellar nucleosynthetic models, the irradiation scenarios are compatible with the conventional hypothesis involving formation of low-mass stars by ambipolar diffusion of magnetic field lines from the prestellar cloud core, thereby leading to its gravitational collapse over a time scale of ~10 Ma. However, a low-energy stellar source, e.g., an ABG star, can inject short-lived nuclei into a cloud core, still allowing the gravitational collapse to be initiated by ambipolar diffusion. Although both stellar nucleosynthetic and irradiation scenarios can produce ^{41}Ca, ^{26}Al, and ^{53}Mn efficiently, the presence of ^{7}Be (Chaussidon et al. 2004), ^{10}Be (McKeegan et al. 2000), and the revised higher estimates of initial $^{60}Fe/^{56}Fe$ (Mostefaoui et al. 2003, 2004, 2005; Tachibana and Huss 2003) in the early solar

system favor a composite scenario. The presence of ^{7,10}Be essentially requires "local" irradiation production, whereas ^{60}Fe could only be produced by stellar nucleosynthesis. In order to identify the most plausible source(s) of ^{26}Al, ^{41}Ca, and ^{53}Mn along with their chronological implications for the formation of the solar system, it is essential to work out appropriate isotopic and dynamical constraints for all the proposed stellar nucleosynthetic and irradiation scenarios.

Among all the short-lived nuclei found to be present in the early solar system, ^{26}Al offers one of the best-studied cases (MacPherson et al. 1995). The inferred widespread presence of ^{26}Al, together with the canonical value of $\sim 5 \times 10^{-5}$ for the initial ^{26}Al/^{27}Al in the early solar system, makes ^{26}Al the most suitable short-lived nuclei to be used as a guidance in deciphering the plausible source(s). This analysis has to be carried out in the context of the constraints posed by the presence of ^{7}Be, ^{10}Be, and ^{60}Fe that require a composite scenario. The present work critically discusses the various stellar nucleosynthesis scenarios for contaminating the early solar system with radioactive nuclei of mean lives $\tau < 10$ Ma, in order to verify which of them can be excluded (or preferred) in light of available constraints.

Stable-Isotope Anomalies in Ca-Al-Rich Inclusions

CAIs from different chondrites are hosts to a wide variety of stable and radiogenic isotopic anomalies (Lee 1988). The most prominent among them are the isotopic anomalies associated with the neutron-rich isotopes of calcium and titanium (Lee et al. 1979; Fahey et al. 1985, 1987a, 1994; Zinner et al. 1986; Fahey 1988; Ireland 1988, 1990; Ireland et al. 1991; Simon et al. 1998; Sahijpal et al. 2000a). The magnitude of these isotopic anomalies is often found to be exceptionally high (>±10‰) in platy hibonite grains (PLACs) from CM meteorites (see, e.g., MacPherson et al. 1995). Certain trends in the stable-isotope anomalies have been observed that appear to correlate with the presence of extinct ^{26}Al in these phases. In addition, there is a correlation between the morphology of the hibonite grains and the isotopic anomalies (Ireland 1988). The main features of the observed trends are:

1. Most of the PLACs have large ^{48}Ca and ^{50}Ti isotopic anomalies with absence/low traces of extinct ^{26}Al and ^{41}Ca.
2. Hibonites within spinel-hibonite spherules (SHIBs) are generally characterized by small (≤±10‰) isotopic anomalies in ^{48}Ca and ^{50}Ti. These inclusions have the canonical value of ^{26}Al/^{27}Al. In general, these inclusions have almost identical trends in radiogenic and stable-isotope anomalies as those found in CAIs from CV and CO chondrites (e.g., MacPherson et al. 1995).
3. The ^{48}Ca and ^{50}Ti isotopic anomalies in CM hibonites as well as in other CAIs appear to be correlated.

In contrast to the CM hibonites, most of the CAIs from CH chondrites exhibit distinct trends in stable and radiogenic isotopic anomalies. These inclusions are characterized by refractory minerals e.g., grossite, hibonite, spinel, perovskite and Ca pyroxenes (MacPherson et al. 1989; Kimura et al. 1993; Weber and Bischoff 1994; Weber et al. 1995; Krot et al. 1999b). Further, these inclusions show no evidence of extensive evaporation and could have formed by direct gas-solid condensation (Weber et al. 1995). These inclusions also escaped low-temperature alterations and thermal metamorphism (Weber et al. 1995). Among the over thirty CAIs from CH chondrites analyzed, for only three inclusions can one infer the canonical value of ^{26}Al/^{27}Al (Kimura et al. 1993; Weber et al. 1995; Krot et al. 1999a; Makide et al. 2004). Most of the remaining inclusions lack traces of ^{26}Al decay. The Ca and Ti isotopic compositions of most of the inclusions are normal, except for four inclusions that have small ^{48}Ca excesses ≤12‰ (Kimura et al. 1993; Weber et al. 1995). In general, CAIs from CH chondrites lack ^{48}Ca and ^{50}Ti isotopic anomalies as well as evidence for ^{26}Al.

Based on the stable-isotope anomalies in ^{48}Ca and ^{50}Ti and radiogenic isotopic anomalies due to extinct ^{26}Al in CAIs from various chondrites, a minimum of three broadly distinct isotopic nebular reservoirs can be identified. These reservoirs are:

1. ^{26}Al-free with anomalous Ca-Ti isotopic composition, characterized by CM PLACs. Within this group, at least four distinct isotopic components of Ti and three distinct isotopic components of Ca are required to explain the observed isotopic spreads in Ti and Ca (Ireland 1990).
2. ^{26}Al-free with normal Ca-Ti isotopic composition, characterized by typical CH CAIs.
3. ^{26}Al-rich with normal Ca-Ti isotopic composition, characterized by CM SHIBs and CV CAIs.

In spite of these isotopic diversities, all the CAIs derived from these three reservoirs have almost identical anomalous oxygen isotopic abundance patterns with respect to the standard mean ocean water (SMOW) oxygen isotopic composition (Fahey et al. 1987b; Virag et al. 1991; Clayton 1993; Wiens et al. 1999; Sahijpal et al. 1999, 2000b; Makide et al. 2004). A relative enrichment of ~50‰ in ^{16}O along the carbonaceous chondrite anhydrous mineral (CCAM) line is generally observed in CAIs (Clayton 1993; Wiens et al. 1999; Scott and Krot 2001). This enrichment could be due to self-shielding in the ultraviolet photodissociation of CO, thereby leading to a relative enrichment of ^{16}O in CO (Clayton 2002) and a relative enrichment of ^{17,18}O in the subsequently produced H_2O reservoirs. This non-mass dependent isotopic fractionation could have occurred in the presolar cloud (Yurimoto and Kuramoto 2004) or in the solar nebula (Lyons and Young 2004; Lyons 2005).

The isotopic records of CAIs indicate that the ^{26}Al-rich and the ^{26}Al-free solar nebula reservoirs, formed either by spatial and/or temporal heterogeneity of ^{26}Al, were identical in oxygen isotopic composition. However, these reservoirs

were distinct in the neutron-rich stable isotopes of Ca and Ti. In the stellar nucleosynthetic scenario, the ^{26}Al-free and the ^{26}Al-rich solar nebula reservoirs will probably represent the presolar cloud composition before and after the injection and thorough mixing of stellar nucleosynthetic products, respectively (Sahijpal and Goswami 1998). The present work analyzes most of the proposed stellar nucleosynthetic sources of ^{26}Al in the context of the associated stable-isotope anomalies and other short-lived nuclei found in early solar system phases. Incorporation of stable isotopes along with the short-lived nuclei in the presolar cloud by supernovae type II has been studied earlier (Olive and Schramm 1982; Schramm and Olive 1982; Wasserburg et al. 1998; Nichols et al. 1999). The present work deals with a comprehensive analysis of the stellar contributions of stable and short-lived nuclei to the presolar cloud in the context of the observed stable-isotope anomalies in CAIs. A wide range of stellar nucleosynthetic sources is analyzed. This includes supernovae type Ia, II, low- and intermediate-mass TP-AGB stars, novae, and single massive and binary stars evolved from the Wolf-Rayet phase to SNIb/c. Preliminary results of this work were reported earlier (Sahijpal 2002a, 2002b; Sahijpal and Soni 2003).

METHODOLOGY

The astrophysical scenario pertaining to the stellar origin of extinct short-lived nuclei involves injection of nucleosynthetic products into the ~1 $M_\odot$ presolar cloud of radius *r*, by an evolved star at a distance *D* (Cameron et al. 1995). In the case of spherically symmetric stellar ejection, a mass fraction *f* ($=\pi r^2/4\pi D^2$), of the stellar ejecta will be incident on the presolar cloud due to geometrical dilution. Further, a mass fraction η of this incident ejecta will finally progress to the central regions of the collapsing presolar cloud core through Rayleigh-Taylor instabilities (Boss and Vanhala 2001; Vanhala and Boss 2002). Detailed numerical simulations of the interaction of shock waves of velocities ~10–45 km s^{-1} with dense molecular cloud cores infer η ~0.1 (Boss and Vanhala 2001; Vanhala and Boss 2002). The net mass fraction of the stellar ejecta that will finally homogenize with a β mass fraction of the presolar cloud would be *F* (= f.η). The parameter β is ~1 in the case the incident stellar ejecta mix with the entire presolar cloud. It will take a value of ~0.01 if the evolved solar protoplanetary disc alone received the incident stellar ejecta (Desch and Ouellette 2005). Let M_{26Al} and M_{27Al} be the total masses of ^{26}Al and ^{27}Al injected by the evolved star, respectively, and $\beta.M_{27Al_\odot}$ be the β mass fraction of the presolar cloud's ^{27}Al before the stellar injection. For an elapsed time *T*, also referred as the free-decay time interval corresponding to the time between the nucleosynthesis of ^{26}Al and the formation of CAIs with the canonical value of 5×10^{-5} for ^{26}Al/^{27}Al in the solar nebula, the mass fraction *F* can be calculated from:

$$\frac{M_{26Al} \times \exp(-T/\tau_{26}) \times F}{(M_{27Al} \times F) + \beta.M_{27Al_\odot}} = 5 \times 10^{-5} \quad (1)$$

The absence or lower abundance of initial ^{26}Al/^{27}Al in several CAIs that have not undergone substantial secondary alterations subsequent to their formation, e.g., CAIs from CH chondrites, PLAC hibonites, indicate either spatial or temporal heterogeneity of ^{26}Al in the solar nebula (MacPherson et al. 1995; Podosek and Nichols 1997; Sahijpal and Goswami 1998). In the stellar nucleosynthetic scenario, the injected stable and short-lived nuclei will finally homogenize with the solar nebula to yield ^{26}Al-rich reservoir of canonical initial ^{26}Al/^{27}Al and normal stable-isotope compositions (Sahijpal and Goswami 1998), except for the observed oxygen isotopic anomalies. As a result, the presolar cloud prior to stellar injection of ^{26}Al would represent the ^{26}Al-free reservoirs with probably anomalous stable-isotope compositions compared to the ^{26}Al-rich reservoirs representing the final normal bulk solar isotopic mix. We have assigned the stable-isotope anomalies to the CAIs formed in the ^{26}Al-free nebula reservoirs compared to CAIs formed in the ^{26}Al-rich nebula reservoirs. For any stable nuclei, e.g., ^{40}Ca, the β mass fraction of the presolar cloud's ^{40}Ca $\beta.M_{40Ca_\odot}$, prior to stellar injection would be represented as:

$$\beta.M_{40Ca_\odot final} \approx \beta.M_{40Ca_\odot final} + (M_{40Ca} \times F) \quad (2)$$

Here, $\beta.M_{40Ca_\odot}$ final is the final β mass fraction of the presolar cloud's ^{40}Ca and M_{40Ca} is the ^{40}Ca mass ejected by the evolved star. If β < 1 (e.g., β ~0.01), Equation 2 will hold only if the second term is small compared to the first on the right hand side. The denominator of the Equation 1 will thus represent $\beta.M_{27Al_\odot final}$. A stable-isotope anomaly associated with CAIs formed in the ^{26}Al-free reservoir(s) with respect to the CAIs formed in the ^{26}Al-rich reservoir in any stable nuclei, e.g., ^{42}Ca, normalized to its most abundant isotope ^{40}Ca, will be represented as:

$$\Delta^{42}Ca(‰) = [(M_{42Ca_\odot}/M_{40Ca_\odot})/(M_{42Ca_\odot final}/M_{40Ca_\odot final}) - 1] \times 1000 \quad (3)$$

The initial ^{41}Ca/^{40}Ca ratio of the CAIs formed in the ^{26}Al-rich reservoir would be:

$$\frac{M_{41Ca}\exp(-T/\tau_{41}) \times F}{\beta.M_{40Ca_\odot final}} \quad (4)$$

The stable-isotope composition of the presolar cloud subsequent to stellar injection and homogenization was taken from Anders and Grevesse (1989) as was the ^{16}O mass abundance. Due to the ambiguity in determining the pristine oxygen isotopic composition of the CAI-forming reservoirs

(Wiens et al. 1999), the final mass fractions of $^{17,18}O$ were calculated using the SMOW oxygen isotopic ratios. The choice of any other oxygen isotopic composition, e.g., a relative enrichment of ^{16}O by 50‰ compared to the SMOW oxygen isotopic composition, will not alter the conclusions. In general, the oxygen isotopic anomalies associated with the ^{26}Al-free reservoirs with respect to the ^{26}Al-rich reservoirs will be represented as:

$$\Delta^{17}O(‰) = [(M_{17O_\odot}/M_{16O_\odot})/(M_{17O_\odot final}/M_{16O_\odot final}) - 1] \times 1000 \quad (5)$$

$$\Delta^{18}O(‰) = [(M_{18O_\odot}/M_{16O_\odot})/(M_{18O_\odot final}/M_{16O_\odot final}) - 1] \times 1000 \quad (6)$$

The deviation, $\delta^{17}O(‰)$, in $^{17}O/^{16}O$ from the terrestrial mass fractionation line is given as:

$$\delta^{17}O = \Delta^{17}O - 0.51 \times \Delta^{18}O \quad (7)$$

Stellar injection into the presolar cloud would result in gradual evolution of the oxygen isotopic composition. An enhanced contribution of either ^{17}O or ^{18}O (i.e., $\Delta^{17}O \neq \Delta^{18}O$) by a stellar source would lead to a systematic observable departure from the observed CCAM line of slope ~1. In the case of CAIs that do not exhibit large mass-dependent isotopic fractionation effects as generally observed in FUN inclusions (e.g., Lee 1988), observed departure(s) from CCAM line could be attributed to the late stage stellar injection. However, for small variations of $\Delta^{17}O$ along the CCAM line it would be difficult to identify the actual cause of isotopic anomalies, as the non-mass dependent isotopic fractionation themselves produce a spread along the CCAM line.

The stellar nucleosynthetic yields of short-lived nuclei along with their most abundant stable nuclei are presented in Table 1. The adopted initial reference values of the various short-lived nuclei in the early solar system are also presented in Table 1. Stellar nucleosynthetic yields of most of these models were taken from the refereed literature except in the case of Wolf-Rayet stars evolved through supernova Ib/c. In the latter case, the nucleosynthetic yields of Wolf-Rayet phases were integrated with the supernova Ib/c yields by making certain approximations.

In order to study the dynamics of the propagation of a stellar shock wave through the intercloud medium (ICM) to the presolar cloud, we estimated the time required and the distance traveled by the shock wave to slow down to ~10 km s^{-1}. The final shock wave velocity of ~10 km s^{-1} would correspond to the minimum velocity required to trigger the gravitational collapse of the presolar cloud (Boss and Vanhala 2001; Vanhala and Boss 2002). Detailed analysis of the interaction of supernova ejecta with the interstellar medium identifies three sequential episodes, i.e., blast wave (constant velocity), Sedov (constant energy), and snow plow (constant momentum). Finally, the stellar shock wave is retarded and dispersed by the random motions of the interstellar medium (see e.g., Padmanabhan 2001). A supernova shock wave can propagate a distance of ~ 40 pc in ~2×10^5 yr prior to merging with the interstellar medium at velocities <10 km s^{-1}. However, the interaction of supernova shock wave with dense regions of molecular clouds can trigger star formation over much shorter distances of <20 pc (e.g., Kothes et al. 2001). We considered the propagation of stellar shock waves for three different density profiles of the ICM, i.e., a) a constant density of 10^{-23} gm cm^{-3}, b) a constant density of 10^{-21} gm cm^{-3}, c) a hypothetical, exponentially increasing density rise from 10^{-24} to 10^{-20} gm cm^{-3} over 10 pc, from the evolved star. The central density of the ~1 $M_\odot$ presolar cloud that can be triggered to gravitational collapse by a stellar shock wave (10–45 km s^{-1}) is assumed to be ~6×10^{-19} gm cm^{-3}, with the cloud's radial dimensions <0.1 pc (Vanhala and Boss 2002). We carried out 1-D (spherically symmetric) analysis of the propagation of stellar shock waves with a spatial grid size of 0.003 pc to estimate the time T_f, and the distance D traveled by the shock wave. Conservation of momentum during the interaction of the stellar shock wave with the ICM was assumed to be the sole cause for the retardation of the shock wave (Cameron 2003). The initial velocities of the shock waves associated with supernova ejecta, Wolf-Rayet winds, and AGB winds were assumed to be 2×10^4, 3×10^3, and 10 km s^{-1}, respectively. The size of the presolar cloud r was inferred from the incident mass fraction f of the stellar ejecta and the distance D.

Stellar Nucleosynthetic Models

Supernovae Type II (SNII)

Supernovae type II models of 11–25 $M_\odot$ stars are considered to be plausible sources of the short-lived nuclei ^{26}Al, ^{60}Fe, ^{41}Ca, ^{36}Cl, ^{53}Mn, and ^{182}Hf. Several groups have estimated SNII yields for a wide range in the treatment of stellar evolution and nucleosynthetic details (Woosley and Weaver 1995; Thielemann et al. 1996; Limongi et al. 2000; Rauscher et al. 2002; Chieffi and Limongi 2004). Among the recent SNII models, Rauscher et al. (2002) predicts the highest ^{26}Al yields. We have used the Rauscher et al. (2002) models of 15–25 $M_\odot$ stars with initial solar metallicity as a reference. However, in order to make a comparative study, we have also analyzed SNII yields recently obtained by Chieffi and Limongi (2004). The SNII yields of the short-lived nuclei obtained by the two groups are presented in Table 1.

In order to understand the influence of the injected mass cut in the supernova explosion on the contributions of short-lived and stable nuclei to the early solar system, we analyzed the isotope source table for the 25 $M_\odot$ SNII with the injected mass cuts at the O/Ne and O/C shells (Meyer et al. 1995).

The inferred stable-isotope anomalies expected in the

Table 1. Stellar nucleosynthetic yields of short-lived nuclei and their most abundant stable nuclei.

Models		Type	^{26}Al	^{27}Al	^{36}Cl	^{35}Cl	^{41}Ca	^{40}Ca	^{53}Mn	^{55}Mn	^{60}Fe	^{56}Fe
ONe1		Nova	1.3(−7)	5.6(−7)								
ONe2–7			0.3–5(−8)	1–24(−8)								
CO1–7			1–6(−10)	0.3–2(−9)								
WDD1–3		SNIa[a]	2–5(−7)	1–4(−4)	0.5–1(−6)	5–9(−5)	4–5(−6)	2–3(−2)	1.5(−4)	6–9(−3)	7.3(−5)	~1.5
CDD1–2			2–3(−7)	2–5(−4)	0.7–1(−6)	7–9(−5)	4–5(−6)	2–3(−2)	9(−5)	7–8(−3)	0.6–3(−7)	~1.1
c3_3d			1(−6)	1(−3)	8(−7)	5(−5)	1(−6)	3(−3)	5(−4)	6(−3)	6(−12)	~0.6
b30_3d			4.5(−6)	5.9(−4)	6.3(−7)	4.6(−5)	2.4(−6)	3.6(−3)	4.8(−4)	6.4(−3)	4.5(−10)	~0.9
1.5 $M_\odot$		AGB	9.0(−7)[b]	4.6(−5)[b]	5.6(−9)[b]	2.0(−6)[b]	2.2(−8)[b]	4.8(−5)[b]			9.3(−9)[b]	9.4(−4)[b]
3 $M_\odot$			1.2[c]–17[b] (−7)	1.4(−7)[c]			4.2(−8)[b]	1.4(−4)[c]			9.2(−8)[b]	2.7(−3)[c]
4 $M_\odot$			1.4(−7)[c]	1.9(−4)[c]								
5 $M_\odot$			4.6[c]–25[b] (−7)	2.5(−4)[c]			4.6(−8)[b]	2.5(−4)[c]			1.5(−5)[b]	4.8(−3)[c]
6 $M_\odot$			4.4(−6)[c]	3.1(−4)[c]								
7 $M_\odot$A		He stars	5.1(−5)	5.2(−3)	2.3(−6)	1.8(−4)	3.2(−6)	2.1(−3)	4.9(−5)	4.4(−4)	8.1(−5)	1.5(−1)
10 $M_\odot$A			6.2(−5)	8.0(−3)	2.7(−6)	2.0(−4)	3.1(−6)	2.4(−3)	8.2(−5)	5.3(−4)	2.4(−5)	1.1(−1)
20 $M_\odot$			4.3(−5)	5.0(−3)	1.4(−6)	1.6(−4)	3.7(−6)	3.4(−3)	1.2(−4)	6.8(−4)	9.6(−5)	1.3(−1)
C13		SNII[d]	1.1(−5)	2.3(−3)	1.4(−6)	9.2(−5)	3.8(−6)	4.0(−3)	9.4(−5)	6.6(−4)	2.3(−6)	2.1(−1)
S15			2.6(−5)	4.7(−3)	1.5(−6)	1.5(−4)	4.3(−6)	6.3(−3)	1.8(−4)	1.3(−3)	6.6(−5)	2.4(−1)
	C15		7.0(−6)	1.7(−3)	2.6(−6)	1.9(−4)	6.4(−6)	8.2(−3)	2.2(−4)	1.4(−3)	9.3(−5)	2.2(−1)
	S19		3.2(−5)	1.0(−2)	2.6(−6)	4.2(−4)	2.7(−5)	1.3(−2)	2.1(−4)	1.5(−3)	1.1(−4)	2.2(−1)
	S20		3.0(−5)	1.2(−2)	1.2(−4)	8.3(−3)	4.3(−4)	2.4(−2)	1.3(−4)	9.9(−4)	3.6(−5)	2.1(−1)
C20			1.5(−5)	1.9(−2)	3.8(−6)	2.1(−4)	1.3(−5)	8.6(−3)	2.1(−4)	1.3(−3)	1.1(−5)	2.2(−1)
S21			4.6(−5)	1.7(−2)	2.8(−6)	2.5(−4)	6.9(−6)	9.3(−3)	2.3(−4)	1.5(−3)	2.5(−5)	2.2(−1)
	S25		7.0(−5)	2.2(−2)	6.9(−6)	6.5(−4)	3.2(−5)	1.7(−2)	3.6(−4)	2.3(−3)	1.5(−4)	2.3(−1)
	C25		2.5(−5)	3.1(−2)	5.7(−6)	4.5(−4)	3.3(−5)	1.6(−2)	2.9(−4)	2.0(−3)	5.0(−5)	2.2(−1)
W60NR		WR	9.5(−5)	4.2(−4)	1.1(−6)	3.9(−5)	7.9(−7)	8.1(−4)	n.d.	n.d.	3(−10)	1.6(−2)
W60R			1.2(−4)	9.4(−4)	n.d.	n.d.	n.d.	n.d.	n.d.	n.d.	n.d.	n.d.
WSNA60		SN1b/c	1.2(−4)	8.0(−2)	4.4(−6)	4.3(−4)	2.4(−5)	2.3(−2)	4.7(−4)	2.0(−3)	1.8(−5)	2.5(−1)
40 $M_\odot$			1.4(−4)	2.8(−2)	3.7(−6)	1.6(−4)	5.4(−6)	1.5(−3)	1.2(−4)	6.8(−4)	9.6(−5)	1.3(−1)
WSNB60			1.7(−4)	2.0(−2)	2.8(−6)	1.6(−4)	4.7(−6)	1.8(−3)	1.2(−4)	6.8(−4)	9.6(−5)	1.3(−1)
85 $M_\odot$			2.0(−4)	1.0(−2)	1.4(−6)	1.6(−4)	3.7(−6)	3.4(−3)	1.2(−4)	6.8(−4)	9.6(−5)	1.3(−1)
120 $M_\odot$			2.7(−4)	1.2(−2)	1.4(−6)	1.6(−4)	3.7(−6)	3.4(−3)	1.2(−4)	6.8(−4)	9.6(−5)	1.3(−1)

[a]WDD1-3 and CDD1-2 (Iwamoto et al. 1999) and c3_3d & b30_3d (Travaglio et al. 2004) are SN1a models.

[b]AGB stars: Busso et al. (2003) and Nollett et al. (2003).

[c]AGB stars: Karakas (2003) and Karakas and Lattanzio (2003).

[d]S15-25 (Rauscher et al. 2002) and C13-25 (Chieffi and Limongi, 2004) are SNII models.

Stellar nucleosynthetic yields (in $M_\odot$) are expressed in base (exponent) form.

Adopted initial reference values of the short-lived nuclei in the early solar system: $^{26}Al/^{27}Al \sim 5 \times 10^{-5}$ (MacPherson et al. 1995); $^{53}Mn/^{55}Mn \sim 2 \times 10^{-5}$ (Birck et al. 1999); $^{41}Ca/^{40}Ca \sim 10^{-8}$ (Srinivasan et al. 1994; Sahijpal et al. 2000a); $^{60}Fe/^{56}Fe \sim (2–20) \times 10^{-7}$ (Mostefaoui et al. 2003, 2004, 2005; Tachibana and Huss 2003); $^{36}Cl/^{35}Cl \sim (0.5–1) \times 10^{-5}$ (Lin et al. 2004; the initial early solar system value was at least $>10^{-4}$); $^{107}Pd/^{108}Pd \sim 4.5 \times 10^{-5}$ (Kelly and Wasserburg 1978); $^{182}Hf/^{180}Hf \sim 2 \times 10^{-4}$ (Kleine et al. 2002).

CAIs formed in the ^{26}Al-free nebular reservoirs are presented in Table 2. In addition, the estimated initial abundance of the various short-lived nuclei at the time of formation of the CAIs with the canonical value of 5×10^{-5} for ^{26}Al/^{27}Al are presented in the table. SNII contributions of the various stable nuclei to the bulk solar system ($\beta \sim 1$) or the solar protoplanetary disc ($\beta \sim 0.01$) are also presented in Table 2. A representative set of data is plotted in Fig. 1. The distance D, traveled by SNII shock wave during time T_f prior to acquiring a final velocity of 10 km s^{-1} for the three density profiles of ICM are estimated in Tables 2 and 3. The inferred radius r, of the presolar cloud is based on the distance D. The major features of the results are:

1. All the SNII models exhibit a wide range of stable-isotope anomalies in the major CAIs forming elements, e.g., Ca, Ti, Mg, Si and O. Most of these anomalies can be well resolved by mass spectrometry. However, none of these anomalies have been observed in CAIs from a wide range of chondrites. In general, compared to the free-decay time interval of 30 yr, the magnitude of the stable-isotope anomalies increases by a factor of 4 and 2 corresponding to the free-decay time interval of 1.5 Ma and 0.8 Ma, respectively. Among all the analyzed SNII models, the S15 and S25 SNII models perform better for a short free-decay time interval of ~30 yr ($\beta \sim 0.01$). This corresponds to the injection of short-lived nuclei into the protoplanetary disk (Desch and Ouellette 2005). In general, SNII yields obtained by Rauscher et al. (2002) produce smaller stable-isotope anomalies than those of Chieffi and Limongi (2004).
2. The SNII model with a mass cut at the O/Ne shell yields relatively small stable-isotope anomalies even for free-decay time interval of 0.8 Ma (Table 2). The isotopic anomalies in O, Ti, and Ca can be further reduced to ≤2‰ for a free-decay time interval of ~30 yr ($\beta \sim 0.01$). However, the Mg isotopic anomalies would still be significant (~−10‰). The inferred initial abundance of the various short-lived nuclei in this scenario would be: ^{41}Ca/^{40}Ca (2×10^{-6}), ^{36}Cl/^{35}Cl (2×10^{-5}), ^{60}Fe/^{56}Fe (2×10^{-7}) and ^{53}Mn/^{55}Mn (3×10^{-8}).
3. For SNII models (Rauscher et al. 2002; Chieffi and Limongi 2004), the yields of ^{53}Mn/^{55}Mn and ^{60}Fe/^{56}Fe are high compared to their calculated initial ratios in the early solar system (Table 2 and Fig. 1). The inferred yields of ^{182}Hf/^{180}Hf and ^{107}Pd/^{108}Pd ratios are within the observed range. However, the inferred initial ^{41}Ca/^{40}Ca is high for free-decay time intervals < 0.8 Ma.
4. If we exclude substantial production of ^{26}Al by SNII, several distant (≥10 pc) SNII scenarios with to a free-decay time interval of ~2 Ma and ^{60}Fe contributions to the early solar system can be postulated. Within an order of magnitude, these stellar scenarios can explain the initial abundance of ^{53}Mn, ^{107}Pd, and ^{182}Hf in the early solar system (Table 3 and Fig. 1). Although one order of magnitude is a large uncertainty, it is not possible to derive more stringent constraints from such a model-dependent scenario. Nonetheless, the possible consequences of these scenarios need to be explored.

Supernovae Type Ia (SNIa)

Supernovae type Ia are the key contributors of Fe-group nuclei to the galaxy. Explosive nucleosynthesis of some of the Chandrasekhar mass SNIa models with slow deflagrations and high central densities of an accreting white dwarf at thermonuclear runaway produces a wide range of neutron-rich Fe-group nuclei, e.g., ^{48}Ca, ^{50}Ti, ^{54}Cr, and ^{54,58}Fe (Iwamoto et al. 1999). These SNIa models could be essential to the understanding of the origin of stable-isotope anomalies in the neutron-rich Fe-group nuclei. In addition, some of the SNIa models produce significant yields of ^{60}Fe, ^{36}Cl, ^{53}Mn, and ^{41}Ca that are comparable to SNII yields (Iwamoto et al. 1999). We analyzed SNIa models with two different central densities, viz, $\rho_c \sim 1.4 \times 10^9$ gm cm^{-3} (C) and 2.1×10^9 gm cm^{-3} (W), of the accreting white-dwarf at thermonuclear runaway, and with different deflagration-to-detonation (DD1-3) transition densities (Iwamoto et al. 1999).

In order to make a comparative study, we also analyzed multi-dimensional hydrodynamical simulations of SNIa recently developed by Travaglio et al. (2004). In contrast to the 1-D SNIa models (Iwamoto et al. 1999) that require parameterization of deflagration speed and the central density (ρ_c) to reproduce a desired SNIa light curve and nucleosynthesis of n-rich Fe-peak nuclei, the multi-dimensional simulations are based on hydrodynamical evolution of the thermonuclear runaway. These simulations were run for a defined initial set of ignition conditions and chemical composition of the accreting white dwarf (Travaglio et al. 2004). We analyzed the 3-D models corresponding to two different choices of ignition conditions, i.e., centrally ignited (c3_3d) and bubbles (off-centered ignited) (b30_3d). Among these hydrodynamical models, the latter has been considered as a standard SNIa model as it leads to more intense nuclear burning in the accreting white dwarf.

The results are presented in Table 4. Even for a very short free-decay time interval of 0.4 Ma, which is required to produce the canonical value of ^{26}Al/^{27}Al in the early solar system, all the SNIa models imply extremely large and unobserved stable-isotope anomalies in Ca, Ti, Mg, Si and O. The inferred initial abundances of all the other short-lived nuclei in the early solar system are orders of magnitude too high except in the case of 3-D hydrodynamical models, which yield low ^{60}Fe/^{56}Fe. The low ^{60}Fe yields in the hydrodynamical models could be due to partial (incomplete) burning during the thermonuclear runaway. The production of ^{60}Fe increases by more than two orders of magnitude by increasing the bubble (ignition point) count from 5 to 30 (Travaglio et al. 2004). Nonetheless, the contribution of ^{60}Fe from hydrodynamical SNIa models requires re-examination.

If we exclude SNIa as the exclusive source of ^{26}Al, there

Table 2. Associated effects in stable and short-lived nuclei for SNII models.

Models[a]	C13	S15		C15	S19		C20	S20	S21	C25	S25		M25[b]	M25[c]
Fraction (F)	6(−4)	3(−4)	2(−4)	8(−4)	2(−4)	9(−7)	4(−4)	2(−4)	1(−4)	2(−4)	1(−4)	4(−7)	6(−5)	1(−4)
Time (T)	8(5)	8(5)	4(5)	8(5)	8(5)	3(1)	8(5)	8(5)	8(5)	8(5)	8(5)	3(1)	8(5)	8(5)
D[d] (pc)	30-8-8	36-8-8	36-8-8	36-8-8	40-9-9	–	40-9-9	40-9-9	40-9-9	40-9-9	40-9-9	–	40-9-9	40-9-9
Time (T_f, in 10^5)	7-2-1	8-2-1	8-2-1	8-2-1	8-2-1	–	8-2-1	8-2-1	8-2-1	8-2-1	8-2-1	–	8-2-1	8-2-1
Radius[e] (r, pc)	5–1	4–0.8	3–0.7	6–1.4	3–0.8	–	4–1	3–0.8	3–0.6	3–0.8	3–0.6	–	2–0.4	3–0.6
$^{36}Cl/^{35}Cl$	4(−5)	2(−5)	4(−5)	1(−4)	3(−5)	9(−5)	9(−5)	1(−3)	2(−5)	8(−5)	4(−5)	1(−4)	6(−5)	5(−6)
$^{41}Ca/^{40}Ca$	2(−7)	8(−8)	8(−7)	4(−7)	4(−7)	4(−5)	4(−7)	7(−6)	7(−8)	6(−7)	2(−7)	2(−5)	1(−8)	3(−8)
$^{53}Mn/^{55}Mn$	3(−3)	3(−3)	2(−3)	1(−2)	3(−3)	2(−3)	5(−3)	2(−3)	2(−3)	4(−3)	2(−3)	1(−3)	5(−8)	3(−8)
$^{60}Fe/^{56}Fe$	7(−7)	8(−6)	7(−6)	4(−5)	1(−5)	8(−6)	2(−6)	4(−6)	2(−6)	6(−6)	7(−6)	5(−6)	3(−7)	5(−8)
$^{107}Pd/^{108}Pd$	n.d.	8(−5)	6(−5)	n.d.	1(−4)	7(−5)	n.d.	8(−5)	2(−4)	n.d.	1(−4)	5(−5)	n.d.	n.d.
$^{182}Hf/^{180}Hf$	n.d.	1(−4)	9(−5)	n.d.	1(−3)	5(−4)	n.d.	2(−4)	3(−4)	n.d.	1(−4)	7(−5)	n.d.	n.d.
^{16}O[f]	18	20	14	45	35	17	55	46	32	57	30	14	20	12
^{25}Mg	22	30	20	25	56	27	100	17	42	77	40	19	26	12
^{26}Mg	25	25	17	44	51	24	91	22	38	88	43	20	27	20
^{27}Al	22	18	13	25	33	16	124	41	37	118	32	15	28	3
^{28}Si	58	34	23	167	46	22	92	135	32	83	46	22	2	3
^{40}Ca	37	24	16	114	40	19	55	80	20	61	24	11	1	3
^{46}Ti	24	14	10	63	61	29	43	186	14	82	35	16	2	3
^{48}Ti	65	13	9	80	15	7	32	22	10	21	8	4	1	3
$\Delta^{17}O$[g]	–8	14	10	10	31	14	43	43	28	50	27	13	3	–26
$\Delta^{18}O$	–82	–19	–13	–142	–5	–2	–63	14	15	14	25	11	5	–21
$\delta^{17}O$	34	24	17	83	33	15	75	35	20	43	14	7	0.4	–16
$\Delta^{25}Mg$	18	–12	–8	31	–34	–16	–1	12	–17	–23	–16	–7	–17	–9
$\Delta^{29}Si$	19	13	9	100	30	14	31	50	7	43	21	10	–5	–0.6
$\Delta^{30}Si$	–13	–10	–7	27	27	13	–8	–8	–19	23	10	4	–5	–1
$\Delta^{42}Ca$	13	7	5	44	–74	–35	7	–532	4	–31	–21	–10	–1	–1
$\Delta^{43}Ca$	19	17	12	100	29	14	13	–250	13	18	16	8	–2	–1
$\Delta^{44}Ca$	–42	19	13	60	34	16	22	59	16	45	21	10	0	0
$\Delta^{48}Ca$	32	21	15	116	39	18	51	83	18	59	23	12	1	3
$\Delta^{49}Ti$	32	–11	–7	–33	–13	–6	–27	–50	–10	–32	–12	–7	–2	–1
$\Delta^{50}Ti$	60	7	5	68	4	2	12	11	0	–0.4	–1	–1	–5	–2

[a]S15-25 (Rauscher et al. 2002) and C13-25 (Chieffi and Limongi 2004) are SNII models.

[b]Mass cut at the O/Ne shell.

[c]Mass cut at the O/C shell (Meyer et al. 1995).

[d]The distance D traveled by the shock waves in time T_f before slowing to a final velocity of 10 km s^{-1} for the three density profiles of the intercloud medium (ICM), i.e., a) a constant density of 10^{-23} gm cm^{-3}, b) a constant density of 10^{-21} gm cm^{-3}, c) an exponentially increasing density rise from 10^{-24} to 10^{-20} gm cm^{-3} over 10 pc from the evolved star. The scenarios with $T < T_f$ are not dynamically feasible. An increase in T ($\geq T_f$) would be essential in these scenarios. This would result in larger stable-isotope anomalies.

[e]Estimated radius r (maximum-minimum) of the presolar cloud based on D and $f = (F/\eta)$, $\eta \sim 0.1$.

[f]Stellar contributions of the stable-nuclei (in ‰) to the bulk solar system composition.

[g]Associated stable-isotope anomalies (in ‰) expected in the CAIs formed in the ^{26}Al-free nebular reservoirs compared to the CAIs formed in the ^{26}Al-rich nebular reservoir.

$\beta \sim 0.01$ for time $T \sim 30$ yr and ~1, otherwise.

The inferred initial abundances of the short-lived nuclei in the early solar system with respect to their stable nuclei abundances, the fraction (F) and the free-decay time interval (T) are expressed in base (exponent) form.

An initial value of 5×10^{-5} for $^{26}Al/^{26}Al$ was assumed in the early solar system.

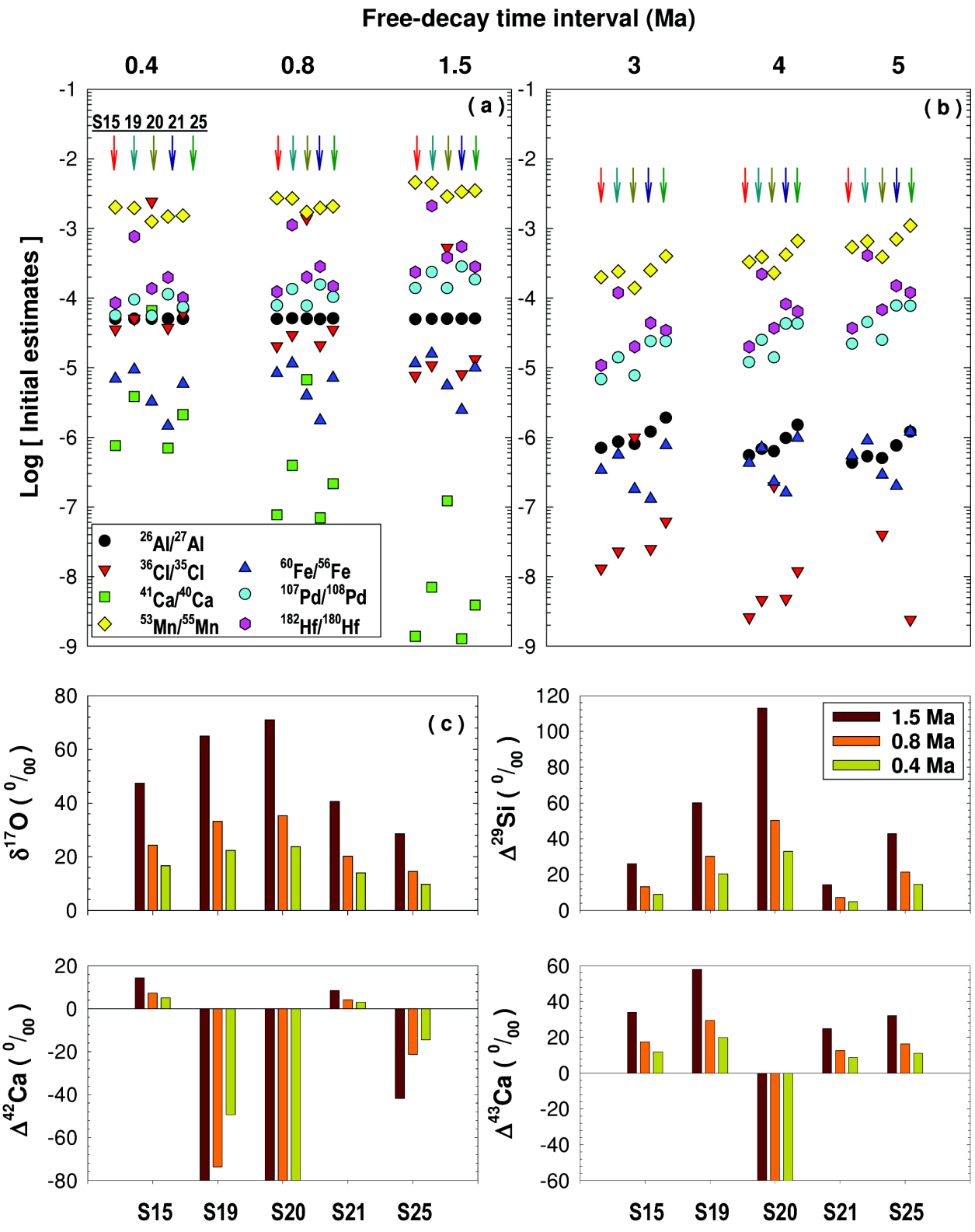

Fig. 1. Initial estimates of the various short-lived nuclei in the early solar system from SNII models corresponding to different free-decay time interval by assuming: a) the canonical value of ~5 × 10^{-5} for $^{26}Al/^{27}Al$, b) an initial value in the range (2–20) × 10^{-7} for $^{60}Fe/^{56}Fe$, and c) the inferred stable-isotope effects in O, Si and Ca isotopes anticipated in CAIs for different free-decay time interval.

Table 3. Associated effects in short-lived nuclei for SNII models.

Models[a]	S15		C15	S19	S20		S25	C25
Fraction (F)	1(−5)	1(−4)	2(−5)	5(−5)	1(−5)	7(−5)	1(−5)	2(−5)
Time (T)	2(6)	4(6)	2(6)	2(6)	2(6)	2(6)	2(6)	2(6)
D[b] (pc)	36-8-8	36-8-8	36-8-8	40-9-9	40-9-9	40-9-9	40-9-9	40-9-9
Time (T_f, in 10^5)	8-2-1	8-2-1	8-2-1	8-2-1	8-2-1	8-2-1	8-2-1	8-2-1
Radius[c] (r, pc)	0.7–0.2	2–0.5	1–0.2	1.8–0.4	0.8–0.2	2–0.5	0.8–0.2	1–0.2
$^{26}Al/^{27}Al$	1(−6)	1(−6)	4(−7)	4(−6)	1(−6)	5(−6)	3(−6)	1(−6)
$^{36}Cl/^{35}Cl$	8(−8)	5(−9)	2(−7)	5(−7)	6(−6)	3(−5)	4(−7)	4(−7)
$^{41}Ca/^{40}Ca$	2(−12)	2(−17)	3(−12)	4(−11)	2(−10)	8(−10)	1(−11)	2(−11)
$^{53}Mn/^{55}Mn$	1(−4)	7(−4)	2(−4)	6(−4)	1(−4)	5(−4)	3(−4)	3(−4)
$^{60}Fe/^{56}Fe$	3(−7)	9(−7)	6(−7)	18(−7)	2(−7)	8(−7)	7(−7)	3(−7)
$^{182}Hf/^{180}Hf$	7(−6)	4(−5)	n.d.	3(−4)	1(−5)	6(−5)	2(−5)	n.d.
$^{107}Pd/^{108}Pd$	4(−6)	2(−5)	n.d.	3(−5)	5(−6)	2(−5)	1(−5)	n.d.

[a]S15-25 (Rauscher et al. 2002) and C13-25 (Chieffi and Limongi, 2004) are SNII models.

[b]The distance D traveled by the shock waves in time T_f before slowing to a final velocity of 10 km s^{-1} for the three density profiles of the ICM.

[c]Estimated radius r (maximum-minimum) of the presolar cloud based on D and $f = (F/\eta)$, $\eta \sim 0.1$, $\beta \sim 1$.

The inferred initial abundances of the short-lived nuclei in the early solar system with respect to their stable nuclei abundances, the fraction (F) and the free-decay time interval (T) are expressed in base (exponent) form.

An initial value in the range $(2–18) \times 10^{-7}$ for the $^{60}Fe/^{56}Fe$ ratio was assumed in the early solar system.

Table 4. Associated effects in stable and short-lived nuclei for SNIa models.

Models[a]	WDD1-3	WDD1-3	CDD1-2	c3_3d	b50_3d
Fraction (F)	1–2.5(−2)	2.5(−5)	1–1.7(−2)	5(−3)	1(−4)
Time (T)	4(5)	2(6)	4(5)	4(5)	4(5)
D (pc)	9-3-7	9-3-7	9-3-7	9-3-7	9-3-7
Time (T_f, in 10^5)	4-0.8-0.8	4-0.8-0.8	4-0.8-0.8	4-0.8-0.8	4-0.8-0.8
Radius (r, pc)	8–2.6	0.3–0.1	7–2.2	4–1.3	0.6–0.2
$^{26}Al/^{27}Al$	5(−5)	1–3(−8)	5(−5)	5(−5)	5(−5)
$^{36}Cl/^{35}Cl$	2–3(−3)	0.5–1(−7)	2(−3)	6–7(−4)	9(−5)
$^{41}Ca/^{40}Ca$	6–10(−5)	3(−12)	6–8(−5)	0.6–1(−5)	2(−6)
$^{53}Mn/^{55}Mn$	1–3(−1)	2(−4)	6–10(−2)	0.2	3(−2)
$^{60}Fe/^{56}Fe$	4–10(−4)	6(−7)	4–30(−7)	2(−11)	3(−10)
^{12}C	20–140	0	30	>500	80
^{16}O	80–150	0	100	200	32
^{22}Ne	10–160	0	40	620	100
^{24}Mg	130–190	0	160	110	13
^{27}Al	70–90	0	80	75–90	9
^{28}Si	>3000	10	~4400	>300	75
^{40}Ca	>4000	10	>5590	>200	54
$\Delta^{17}O$	80–150	0	110	250	33
$\Delta^{18}O$	90–180	0	110	250	33
$\Delta^{25}Mg$	140–230	0	180	110	6
$\Delta^{29}Si$	~−1300	10	~−1240	>400	65
$\Delta^{30}Si$	~−1100	10	~−1150	200	48
$\Delta^{42}Ca$	−90	6–10	~−100	140	21
$\Delta^{48}Ca$	−100	7–12	~−100	>250	58
$\Delta^{47}Ti$	< −1100	~8	>−1380	410	68
$\Delta^{50}Ti$	>7000	~−50	−870–670	420	70
$\Delta^{54}Cr$	>6000	~−80	−150–3500	>1900	140

[a]WDD1-3 and CDD1-2 (Iwamoto et al. 1999) and c3_3d and b30_3d (Travaglio et al. 2004) are SNIa models.

The first and the last three columns correspond to the canonical value of $^{26}Al/^{27}Al$ in the early solar system, whereas the second column corresponds to an initial value of 6×10^{-7} for the $^{60}Fe/^{56}Fe$ ratio in the early solar system.

can be numerous scenarios corresponding to WDD1-3 models (Iwamoto et al. 1999) with free-decay time interval ~2 Ma that can contribute ^{60}Fe and ^{53}Mn to the early solar system within an order of magnitude (Table 4). The same cautions already mentioned for SNIIe are also applicable here, and one cannot derive more quantitative constraints.

Classical Novae

Several CO and ONe nova models have been analyzed in the present work. These models are based on distinct initial masses of the accreting white dwarf and different levels of mixing between the accreted envelope and the underlying white dwarf core (José and Hernanz 1998). Except for the comparatively massive ONe white dwarfs, most of the classical nova models fail to attain high temperatures for significant nucleosynthesis of elements beyond silicon. In general, among all the extinct short-lived nuclei, classical novae are known to produce ^{26}Al alone.

Even for a short free-decay time interval of ≤0.2 Ma, the various CO nova models cannot contaminate more than 4–20% of the presolar cloud with ^{26}Al to produce the canonical value of 5×10^{-5} for ^{26}Al/^{27}Al in the contaminated fraction. The contamination would result in significant contributions of ^{13}C, ^{15}N and ^{17}O in the range of 120–3000, 60–700, and 300–1000‰, respectively, to the 0.04–0.2 mass fraction of the presolar cloud. The associated oxygen isotopic anomalies expected for the CAIs formed in the ^{26}Al-free nebular reservoirs would be $\delta^{17}O \sim \Delta^{17}O \sim -(300–1000)$‰. The mixing of CO nova ejecta with the entire ~1 $M_\odot$ presolar cloud would result in lower ^{26}Al/^{27}Al ratio in the early solar system compared to its canonical value. This is essentially due to the extremely small ejection of ^{26}Al by CO novae (Table 1).

The various ONe nova models, except for the model ONe1, corresponding to a free-decay time interval of ≤0.2 Ma would contribute ^{15}N and ^{17}O, in the range, 10–120 and 20–70‰, respectively, to the presolar cloud. The associated oxygen isotopic anomalies expected for the CAIs formed in the ^{26}Al-free nebular reservoirs would be $\delta^{17}O \sim \Delta^{17}O \sim -(20–70)$‰. The ONe2 and ONe6–7 novae do not produce enough ^{26}Al to contaminate the entire ~1$M_\odot$ presolar cloud. The remaining ONe models (José and Hernanz 1998) can contribute higher yields of ^{26}Al to the presolar cloud. The model ONe1 yields the lowest stable-isotope anomalies ($\Delta^{17}O \sim \delta^{17}O \sim -6$‰). ONe1 would contribute ~2‰ of ^{15}N to the presolar cloud.

Wolf-Rayet (WR) Stars and Supernovae Type I b/c (SNIb/c)

Single massive stars ($M_{ZAMS} \geq 30\ M_\odot$) of solar metallicity and less massive primary stars ($M_{ZAMS} \geq 15\ M_\odot$) in close binary systems are considered to be the progenitors of SNIb/c (Woosley et al. 1993, 1995, 2002; Cameron et al. 1995; Cerviño et al. 2000; Nomoto et al. 2001a). In the former case, stars going through the Wolf-Rayet (WR) phase lose their entire hydrogen-rich and helium-rich envelops during the WN and WC/WO stages, respectively, and are left with CO cores that finally collapse to SNIb/c. However, in close binary systems, the primary star (the more massive of the two) upon leaving the main sequence loses its entire hydrogen-rich envelope to its companion and turns into a helium star. Additional mass loss as WR winds during core helium burning finally results in the formation of a CO core, the progenitor of SNIb/c (Woosley et al. 1995). We have analyzed the plausible role of SNIb/c from both single massive Wolf-Rayet stars and Wolf-Rayet stars in close binary systems. The free-decay time interval of short-lived nuclei in all the WR + SNIb/c models was taken from the time of SNIb/c explosion.

Wolf-Rayet (WR) Stars in Close Binary Systems: The massive helium stars (≥7 $M_\odot$) in close binary systems eject WR winds over a time scale of ≤1 Ma prior to SNIb/c explosion (Woosley et al. 1995). These stars eject 50% of their masses around 0.5–0.6 Ma prior to SNIb/c explosion. However, in the case of 4 and 5 $M_\odot$ helium stars, WR winds are ejected over a time scales of ~1.4 and 2.0 Ma, respectively, prior to SNIb/c explosion. Due to the delay between the WR and SNIb/c stages, the major He-burning nucleosynthetic products, i.e., ^{12}C, ^{18}O, and ^{22}Ne would be injected at least ~0.5–1 Ma prior to the injection of the final SNIb/c nucleosynthetic products. It is quite likely that the initial WR winds alone trigger the gravitational collapse of the presolar cloud. This could be subsequently followed by the injection of SNIb/c nucleosynthetic products. As ^{26}Al is exclusively produced during SNIb/c in binary WR stars, the expected stable-isotope anomalies in CAIs would be essentially due to SNIb/c. However, there could be contributions to isotopic anomalies from WR winds depending upon how early these winds arrived and were homogenized with the presolar cloud. We have analyzed the plausible isotopic effects due to contributions of WR winds and SNIb/c to the presolar cloud taking into account the dynamics involved in the propagation of shock waves through the ICM (see the footnotes to Table 5 for details).

The results are presented in Table 5. The low-mass helium stars (<7 $M_\odot$) exhibit large stable-isotope anomalies. In the case of massive helium stars (≥7 $M_\odot$), the earlier injected WR winds will contribute ^{12}C, ^{18}O, and ^{22}Ne to the presolar cloud. These isotopes may homogenize with the presolar cloud prior to the injection of ^{26}Al by SNIb/c. This can reduce the stable-isotope anomalies associated with ^{18}O. In general, the inferred isotopic anomalies in other stable isotopes are small compared to those inferred from SNII models for identical free-decay time intervals (Table 2). All the WR + SNIb/c models produce the correct amounts of other short-lived nuclei, except for a too-high initial ^{53}Mn/^{55}Mn ratio. If we exclude significant contributions of ^{26}Al from these stellar sources, the contributions of ^{60}Fe and ^{53}Mn to the presolar cloud become more reasonable, but the early solar system data can only be matched within an order of magnitude (Table 5).

Table 5. Associated effects in stable and short-lived nuclei for SNIb/c models evolved from Wolf-Rayet stars in close binary systems.

He stars	4 $M_\odot$	5 $M_\odot$	7 $M_\odot$A	10 $M_\odot$A	20 $M_\odot$	4 $M_\odot$	7 $M_\odot$A	20 $M_\odot$
Fraction (F)	1(–3)	1.7(–4)	1(–4)	5(–5)	1(–4)	2(–4)	2.5(–5)	2(–5)
Time (T)	4(5)	4(5)	4(5)	4(5)	4(5)	3(6)	2(6)	2(6)
D_{WR}[a] (pc) (50%[a] WR)	9-**2-5**	9-**2-5**	10-2-**5**	11-2-**6**	15-**4-7**	9-**2-5**	10-2-**5**	15-**4-7**
Time (50%[a] WR) ($T_{f\text{-}WR}$, in 10^5)	2-**0.5-0.7**	2-**0.5-0.7**	2-0.5-**0.7**	3-0.6-**0.7**	3-**1-0.9**	2-**0.5-0.7**	2-0.5-**0.7**	4-**1-0.9**
Radius[b] (r, pc)	**0.8–0.4**	**0.5–0.2**	**0.5**	**0.3**	**0.4–0.2**	**0.4–0.2**	**0.2**	**0.2–0.1**
D_{SN}[c] (pc) (SNIb/c)	14-**3-5**	14-**3-5**	17-4-**6**	18-4-**7**	18-**4-7**	14-**3-5**	17-4-**6**	18-**4-7**
Time (SNIb/c) ($T_{f\text{-}SN}$, in 10^5)	4-**1-1**	4-**1-1**	4-1-**1**	4-1-**1**	4-**1-1**	4-**1-1**	4-1-**1**	5-**1-1**
$^{26}Al/^{27}Al$	5(–5)	5(–5)	5(–5)	5(–5)	5(–5)	1(–6)	3(–6)	2(–6)
$^{36}Cl/^{35}Cl$	3(–5)	1(–5)	3(–5)	3(–5)	2(–5)	2(–8)	2(–7)	8(–8)
$^{41}Ca/^{40}Ca$	1(–6)	4(–7)	3(–7)	2(–7)	4(–7)	9(–15)	2(–12)	1(–12)
$^{53}Mn/^{55}Mn$	2(–3)	2(–3)	3(–4)	4(–4)	8(–4)	2(–4)	7(–5)	1(–4)
$^{60}Fe/^{56}Fe$	8(–6)	5(–6)	4(–6)	1(–6)	6(–6)	6(–7)	6(–7)	5(–7)
^{12}C	24	9	14	29	96	6	5	17
^{18}O	82	30	25	22	84	19	8	15
^{22}Ne	25	8	14	33	155	6	5	27
^{28}Si	24	11	10	9	14	6	3	2
$\Delta^{17}O$	2	2	3	5	~7			
$\Delta^{18}O$	–79	–27	-21^{μ}–2^{δ}	-17^{μ}–5^{δ}	-76^{μ}–7^{δ}			
$\Delta^{29}Si$	13	6	3	–1	7			
$\Delta^{30}Si$	4	–3	–7	–10	–3			
$\Delta^{43}Ca$	8	6	1	2	4			
$\Delta^{48}Ca$	12	8	3	3	5			
$\Delta^{47}Ti$	27	11	5	4	6			
$\Delta^{50}Ti$	29	12	5	4	6			

[a]The distance D_{WR} traveled by the shock waves associated with the injection of >50% of Wolf-Rayet wind during time $T_{f\text{-}WR}$ before slowing to a final velocity of 10 km s^{-1} for the three density profiles of the ICM.

[b]Estimated radius r (maximum-minimum) of presolar cloud for $D_{WR} \sim D_{SN}$, $\eta \sim 0.1$, $\beta \sim 1$.

Scenarios marked with bold letters correspond to $D_{WR} \sim D_{SN}$, and may result in initiation of the collapse of the presolar cloud by the WR winds prior to the arrival of SNIb/c shock waves. This may result in lower values of $|\delta^{18}O|^{\delta}$ as ^{18}O injected by the WR phase may get homogenized earlier with the presolar cloud prior to the injection of ^{26}Al by SNIb/c. For the remaining scenarios, the SNIb/c shock wave will sweep up the WR winds to the presolar cloud. This will result in higher values of $|\delta^{18}O|^{\mu}$.

[c]The distance D_{SN} traveled by the SNIb/c shock waves during time $T_{f\text{-}SN}$ before slowing to a final velocity of 10 km s^{-1} for the three density profiles of the ICM. For simplifications, the density profile of the ICM was assumed to be unperturbed by the earlier passage of WR winds prior to SNIb/c. This would result in underestimating D_{SN} as the WR winds will sweep up the ICM, thereby, reducing its density.

Single Massive Wolf-Rayet (WR) Stars: In the case of single massive Wolf-Rayet stars, the nucleosynthetic yields of non-rotating (W60NR) as well as rotating (W60R) models of 60 $M_\odot$ ($Z_\odot$) WR star were obtained from the mean enhancement factors of the various nuclei (Meynet et al. 2001). These yields are based on the recently revised mass-loss rates that take into account WR wind clumping effects. Ejected yields of non-decayed ^{26}Al obtained by the same group with identical models (Knödlseder et al. 2002) were used in deducing the associated stable-isotope anomalies. These ^{26}Al yields are lower than those obtained without including WR wind clumping effects (Meynet et al. 1997). To understand the effect of stellar rotation on the nucleosynthetic yields of WR stars, we analyzed the W60NR and W60R models for their possible contributions to the presolar cloud. However, since the WR stars finally evolve through SNIb/c (Woosley et al. 2002), two models dealing with the WR + SNIb/c nucleosynthetic yields of short-lived and major stable isotopes for the 60 $M_\odot$ star were produced. These models correspond to different mass-loss evolutionary details.

The model (WSNA60) was produced using the recently revised mass-loss rates that take into account WR wind clumping effects (Meynet et al. 2001). The nucleosynthetic yields from the W60NR model were taken for the WR phase. WSNA60 will lose ~14 $M_\odot$ during the entire WR phase (~6 $M_\odot$ and 8 $M_\odot$ mass-loss during the WN and WC/WO phases, respectively). The star will finally evolve into an ~15 $M_\odot$ He star, with ~11 $M_\odot$ CO core at the end of He-burning. In the absence of any suitable model for an evolved ~15 $M_\odot$ He star with ~11 $M_\odot$ CO core, we adopted the SNIb/c model (CO138E1) of a 13.8 $M_\odot$ CO star for the major stable isotopes (Nakamura et al. 2001a). The CO138E1 model was evolved from a 40 $M_\odot$ main sequence star that would finally produce a 16 $M_\odot$ He star. The SNIb/c yields of

the major stable isotopes of the 16 $M_\odot$ He star (Nakamura et al. 2001b) are almost identical to the CO138E1 model yields. The SNIb/c yields of short-lived nuclides of the 16 $M_\odot$ He star, corresponding to an explosive energy of 10^{51} ergs, were taken from Nakamura et al. (2001b). The production of the short-lived nuclides essentially takes place in the final 13.8 $M_\odot$ CO core collapse. A comparative analysis of the W60NR model combined with either 16 or 10 $M_\odot$ He stars that finally evolve to ~13.8 and 8 $M_\odot$ CO cores, respectively, suggests that the choice of 13.8 for the 11 $M_\odot$ CO will not have a large influence on the inferred stable-isotope effects. However, the yields of short-lived nuclei can be affected by up to a factor of two. An average time span of 0.4 Ma was assumed between the injection of ^{26}Al during the WN and SNIb/c stages. The production of ^{60}Fe is invariably low in all the SNIb/c models (Nakamura et al. 2001b) compared to those reported by the same group (Nomoto et al. 2001b; personal communication). In the present work, we took the ^{60}Fe yields from the latter models.

An alternative model (WSNB60) was produced based on the previously used mass-loss rates (uncorrected wind clumping effects). In this scenario, a single 60 $M_\odot$ star will evolve to a ~23 $M_\odot$ mass-losing He star. This star will finally undergo a SNIb/c explosion because of core collapse of Mf ~4.5 $M_\odot$ (Woosley et al. 1995). In the absence of nucleosynthetic yields of an M_f ~4.5 $M_\odot$ core collapse supernova, the yields of a 60 $M_\odot$ WR star (Meynet et al. 1997) were integrated with the M_f ~4.5 $M_\odot$ SNIb/c yields obtained by extrapolating the SNIb/c yields of M_f ~ 2.82, 3.20, 3.51, and 3.55 $M_\odot$ models (Woosley et al. 1995). Even though there will be uncertainties associated with the extrapolation, the ^{26}Al yield of WR + SNIb/c will not be uncertain by more than a factor of 2 as ^{26}Al is mostly ejected during the WN stage. A time interval of 0.4 Ma was assumed between the WN and SNIb/c stages.

In addition to the 60 $M_\odot$ WR star, we have also analyzed M_{ZAMS} ~40, 85, 120 $M_\odot$ WR stars with the previously used mass-loss rates (Meynet et al. 1997; personal communication). These WR stars will finally evolve to M_f ~5, 3.6, 3.6 $M_\odot$, respectively. In the case of 85 and 120 $M_\odot$ WR stars, we used the SNIb/c models corresponding to 20 $M_\odot$ mass-losing He stars that finally evolve to Mf ~3.55 $M_\odot$ (Woosley et al. 1995). However, in the case of the 40 $M_\odot$ WR star, in the absence of a SNIb/c model for Mf ~5 $M_\odot$, we integrated the 40 $M_\odot$ WR yields with the Mf ~5 $M_\odot$ SNIb/c yields obtained by extrapolating the yields of Mf ~2.82, 3.20, 3.51, and 3.55 $M_\odot$ (Woosley et al. 1995).

The results obtained from the analysis of single massive WR + SNIb/c stars are presented in Table 6. W60NR and W60R corresponding to a single 60 $M_\odot$ star exhibit enrichments in the major He-core burning products. The W60R model, which incorporates stellar rotation, yields considerably lower enrichments in ^{12}C and ^{22}Ne because of its higher ^{26}Al production (Knödlseder et al. 2002).

The WSNA-B (non-rotating, WR + SNIb/c) models dealing with different stellar wind mass-loss rates exhibit stable isotope enrichments in both He-core burning products and CO core-collapse products that are predominant in the WSNB and WSNA models, respectively. The WR + SNIb/c models corresponding to 40, 85, and 120 $M_\odot$ stars exhibit enrichments in He-core burning products. These models, along with the WSNB model, exhibit comparatively small isotopic anomalies, specifically in the oxygen isotopes. However, the inferred oxygen isotopic anomalies spread out along the CCAM line on the conventional oxygen isotopic plot. It would be difficult to decipher the cause of these isotopic anomalies as the non-mass dependent isotopic fractionation itself produces a spread along the CCAM line. Except for an order of magnitude high initial ^{53}Mn/^{55}Mn, all other short-lived nuclei can be produced with the right ratios by these stars. The overproduction of ^{53}Mn would be one of the major shortcomings of the stellar scenarios involving SNIb/c, unless circumvented by an appropriate mass cut in the supernova.

Low- and Intermediate-Mass Asymptotic Giant Branch (AGB) Stars

Detailed nucleosynthetic evolution of all the stable nuclei from H to Si along with the short-lived nuclei, ^{26}Al, for 1–6.5 $M_\odot$ TP-AGB stars have been recently computed (Karakas 2003; Karakas and Lattanzio 2003). Unlike some of the earlier estimates of TP-AGB nucleosynthesis based on extrapolation of synthetic models (e.g., Forestini and Charbonnel 1997), the nucleosynthetic yields obtained by Karakas (2003) are based on comprehensive stellar evolutionary models. These TP-AGB models incorporate hot bottom burning processes for ≥5 $M_\odot$ TP-AGB stars of solar metallicity. However, the cool bottom processes were not incorporated for ≤3 $M_\odot$ TP-AGB stars. For the intermediate-mass, 3–6 $M_\odot$ TP-AGB stars of solar metallicity, we adopted the nucleosynthetic yields of ^{26}Al and stable nuclei obtained by Karakas (2003). In addition, we used the recently computed 3 and 5 $M_\odot$ TP-AGB stellar models (Busso et al. 2003) for their possible contributions of ^{41}Ca, ^{26}Al, ^{60}Fe, and ^{107}Pd to the early solar system. These stellar models are based on neutron exposures produced by the ^{22}Ne(α, n)^{25}Mg reaction in the convective pulses, without the inclusion of the ^{13}C(α, n)^{16}O neutron source (Busso et al. 2003). The absolute yields of the short-lived nuclides for the 3 and 5 $M_\odot$TP-AGB stellar models were obtained based on the estimated yields of their most abundant stable nuclides that remain unaltered during the TP-AGB stage. The ^{26}Al yields of the 3 and 5 $M_\odot$ TP-AGB stars obtained by Busso et al. (2003) are markedly different from those obtained by Karakas and Lattanzio (2003). The differences are related to different choices adopted in the two stellar evolution codes for mass loss rates and for defining the convective borders; this last choice affects the extension of dredge-up. None of the 3 $M_\odot$ TP-AGB stellar models incorporates cool bottom processes (Busso et al. 2003).

Table 6. Associated effects in stable and short-lived nuclei for rotating and non-rotating WR models and single massive WR + SNIb/c models.

	W60NR	W60R	WSNA60		40 $M_\odot$	WSNB60		80 $M_\odot$	120 $M_\odot$
Fraction (F)	5(−5)	5(−5)	5(−5)	3(−5)	5(−5)	3(−5)	2(−5)	2(−5)	2(−5)
Time (T)	8(5)	8(5)	8(5)	4(5)	8(5)	8(5)	4(5)	8(5)	8(5)
D (pc)	20-4-7	25-5-8	40-8-9	40-8-9	25-6-8	30-6-8	30-6-8	32-7-8	40-7-8
Time (T_f, in 10^5)	5-1-0.8	6-1-0.8	10-2-0.9	10-2-0.9	6-2-0.9	7-2-0.9	7-2-0.9	8-2-0.9	10-2-0.9
Radius (r, pc)	0.9–0.2	1–0.2	1.8–0.4	1.4–0.3	1–0.3	1–0.2	0.8–0.2	0.8–0.2	1–0.2
$^{26}Al/^{27}Al$	5(−5)	5(−5)	5(−5)	5(−5)	5(−5)	5(−5)	5(−5)	5(−5)	5(−5)
$^{36}Cl/^{35}Cl$	4(−6)	n.d.	1(−5)	2(−5)	1(−5)	6(−6)	1(−5)	2(−6)	2(−6)
$^{41}Ca/^{40}Ca$	4(−9)	n.d.	1(−7)	1(−6)	2(−8)	1(−8)	1(−7)	8(−9)	7(−9)
$^{53}Mn/^{55}Mn$	n.d.	n.d.	2(−3)	1(−3)	3(−4)	3(−4)	2(−4)	2(−4)	2(−4)
$^{60}Fe/^{56}Fe$	1(−11)	n.d.	5(−7)	5(−7)	2(−6)	2(−6)	2(−6)	2(−6)	1(−6)
^{12}C	50	15	41	28	51	72	50	21	10
^{16}O	8	1	53	36	14	11	8	3	2
^{22}Ne	74	36	58	40	73	116	81	39	14
^{24}Mg	1	2	50	35	11	9	6	5	4
^{27}Al	1	1	69	47	21	12	9	5	5
^{28}Si	1	3	41	28	16	10	7	4	3
^{40}Ca	1	n.d.	19	13	1	1	0.7	2	1
$\Delta^{17}O$	8	1	56	38	13	10	7	2	1
$\Delta^{18}O$	9	–4	56	38	13	10	7	–3	2
$\delta^{17}O$	4	3	27	18	6	4	3	4	0
$\Delta^{25}Mg$	–1	1	52	35	5	4	3	0.6	1
$\Delta^{29}Si$	0	2	41	28	–10	–3	–2	2	2
$\Delta^{30}Si$	0	–1	41	28	–13	–8	–6	–1	–1
$\Delta^{42}Ca$	0	n.d.	18	13	~0	~0	~0	0.7	0.5

A single case of a low-mass 1.5 $M_\odot$ TP-AGB star was studied using the stellar models that incorporate cool bottom processes (Nollett et al. 2003). In the absence of absolute yields of the various stable and short-lived nuclei, the ^{16}O and ^{27}Al yields of 1.5 $M_\odot$ TP-AGB star were estimated using a solar mass fraction of these nuclei in an assumed ~0.8 $M_\odot$ envelope ejected during the TP-AGB stage. The abundances of ^{16}O and ^{27}Al remain almost unaltered during the evolution of TP-AGB stars (Forestini and Charbonnel 1997; Karakas 2003; Karakas and Lattanzio 2003; Nollett et al. 2003). Our estimated yields of ^{16}O and ^{27}Al are identical to those obtained by Karakas (2003) for the 1.5 $M_\odot$ TP-AGB star. Based on these yields, the yields of ^{12}C, $^{17,18}O$, ^{14}N, and ^{26}Al were calculated for wide range in the parameters including the mass circulation rate (M[dot]$_\odot$/yr) and the maximum temperature (T_P) experienced by the circulating material in cool bottom burning (Nollett et al. 2003). The yields of the short-lived nuclides ^{41}Ca, ^{36}Cl, ^{60}Fe, and ^{107}Pd were obtained from Busso et al. (2003). A value of 2×10^{-2} corresponding to $T_P \sim 5 \times 10^7$ K was assumed for $^{26}Al/^{27}Al$ (Busso et al. 2003).

The results are presented in Table 7. The 3–5 $M_\odot$ TP-AGB stellar models (Karakas 2003) imply significant contributions of C, O, N, and Ne isotopes to the early solar system, with a prominent isotopic anomaly in ^{17}O. An identical conclusion can be drawn from the semi-analytical models of TP-AGB stars developed by Forestini and Charbonnel (1997). In the case of the 3 $M_\odot$ TP-AGB stellar model, an enhancement in the ^{26}Al yields by a factor of ~10 (Busso et al. 2003) can reduce the inferred stable-isotope effects (Table 7). Further enhancement in the ^{26}Al yields due to incorporation of cool bottom processes for the 3 $M_\odot$ TP-AGB star can reduce the stable-isotope effects substantially. The 1.5 $M_\odot$ TP-AGB model gives small stable-isotope anomalies compared to those of any other stellar source. Increase in $^{26}Al/^{27}Al$ for $T_P > 5 \times 10^7$ K (Nollett et al. 2003) will further reduce the magnitude of stable-isotope anomalies. In spite of significant contributions of ^{41}Ca and ^{107}Pd to the early solar system, the 1.5 $M_\odot$ TP-AGB model cannot produce the required $^{60}Fe/^{56}Fe$ ratio (Busso et al. 2003). However, the $^{60}Fe/^{56}Fe$ ratio in the case of the 3 $M_\odot$ TP-AGB model is within the adopted initial early solar system value (Table 1). The TP-AGB stars in the mass range 1.5–3 $M_\odot$ could be contributors of short-lived nuclei to the early solar system (Busso et al. 2003). When this paper was in the final review stage, we became aware of new models presented by Wasserburg et al. (2006) for AGB stars covering the metallicity range from one-third solar to solar. In these very recent models, which include cool bottom processes above the H burning shell, it was shown that the apparent

Table 7. Associated effects in stable and short-lived nuclei for TP-AGB stars.

	1.5 $M_\odot$[a] $10^{-7.2}$ $M[dot]_\odot$/yr[c]	1.5 $M_\odot$[a] $10^{-5.6}$ $M[dot]_\odot$/yr[c]	3 $M_\odot$[b]	3 $M_\odot$[a]	4 $M_\odot$[b]	5 $M_\odot$[b]	5 $M_\odot$[a]	6 $M_\odot$[b]
Fraction (F)	6(−3)	6(−3)	3(−2)	2(−3)	3(−2)	9(−3)	2(−3)	9(−4)
Time (T)	7(5)	7(5)	4(5)		4(5)	4(5)		4(5)
D[d] (pc)	2.3-0.5-2.6	2.3-0.5-2.6	3.5-0.7-3.2		3.8-0.8-3.3	4-0.8-3.6		4.4-0.9-3.7
Time (T_f, in 10^5)	7-2-7	7-2-7	10-2-8		10-3-8	10-3-9		10-3-9
Radius (r, pc)	1.3–0.24	1.3–0.24	3.8–0.8	1–0.2	4–0.9	2.4–0.5	1.1–0.2	0.8–0.2
$^{26}Al/^{27}Al$	5(−5)	5(−5)	5(−5)		5(−5)	5(−5)		5(−5)
$^{41}Ca/^{40}Ca$	2(−8)	2(−8)	1(−7)			9(−8)		
$^{36}Cl/^{35}Cl$	2(−6)	2(−6)						
$^{60}Fe/^{56}Fe$	3(−8)	3(−8)	2(−7)			2(−5)		
$^{107}Pd/^{108}Pd$	4(−5)	4(−5)	6(−5)			2(−3)		
^{12}C	23	8	230		211	45		2
^{13}C	n.d.	n.d.	180		240	555		19
^{14}N	21	63	180		240	140		36
^{16}O	5	5	73		86	33		4
^{17}O	14	14	550		520	140		24
^{22}Ne	n.d.	n.d.	560		422	96		5
^{27}Al	n.d.	n.d.	80		93	37		5
$\Delta^{17}O$	−9	−9	−510		−476	−108		−20
$\Delta^{18}O$	1	5	~0		~0	~0		~0
$\delta^{17}O$	−10	−12	−510		−476	−108		−20

[a]TP-AGB stellar models (Busso et al. 2003).
[b]TP-AGB stellar models (Karakas A. I. 2003; Karakas A. I. and Lattanzio J. C. 2003)
[c]Models with two different mass circulation rates (Nollett et al. 2003).
[d]Distance traveled by AGB winds during the time T_f before attaining a velocity of ~1 km s^{-1} for the three density profiles of the ICM.

shortage of ^{60}Fe by low-mass AGB stars can be overcome for stars of metallicity slightly lower than solar, yielding $^{60}Fe/^{56}Fe$ ratios up to the highest values inferred for the early solar system (10^{-6}) and still reproducing the concentrations of ^{26}Al, ^{41}Ca, ^{107}Pd, and ^{205}Pb. The very high ^{36}Cl abundance was instead ascribed to energetic particle irradiation.

DISCUSSION

The results obtained from the present work are summarized in Table 8. In order to produce the canonical value of $^{26}Al/^{27}Al$ in the early solar system most of the stellar sources contribute stable nuclei to the presolar cloud. The "late" stage contribution of stable and short-lived nuclei eventually results in the formation of a ^{26}Al-rich nebular reservoir with the canonical value of $^{26}Al/^{27}Al$ and the final bulk solar isotopic composition. This could result in a measurable amount of stable-isotope anomalies in the CAIs formed in the ^{26}Al-free nebula reservoirs compared to the CAIs formed in the ^{26}Al-rich reservoir. Most of the SNIa, SNII, WR + SNIb/c stellar models produce isotopic anomalies in O, Mg, Si, Ca, and Ti, the major elemental constituents of CAIs. The intermediate-mass (3–5 $M_\odot$) TP-AGB stars and novae would contribute C, N, and O isotopes to the presolar cloud. These stellar sources could result in isotopic anomalies in ^{17}O. In summary, we expect isotopic anomalies in O, Mg, Si, Ca and Ti in case ^{26}Al was synthesized by a massive star and ^{17}O isotopic anomalies in case an intermediate-mass TP-AGB star or a nova synthesized ^{26}Al.

Stable-Isotope Constraints on the Stellar Contribution of ^{26}Al

None of the inferred stable-isotope anomalies in O, Mg, Ca, and Ti have been yet observed in the isotopic studies of CAIs from different chondrites (Fahey et al. 1985, 1987a, 1987b, 1994; Zinner et al. 1986; Ireland 1988, 1990; Ireland et al. 1991; Virag et al. 1991; Kimura et al. 1993; Weber et al. 1995; Simon et al. 1998; Sahijpal et al. 1999, 2000a, 2000b). Within the stellar nucleosynthetic scenario there seems to be four possible explanations for the absence of inferred stable-isotope anomalies in the CAIs formed in the ^{26}Al-free solar nebular reservoirs:

1. CAIs from CH chondrite and PLAC hibonites from CM chondrites either formed or attained isotopic closure in Ca, Ti, Si, Mg, and O against thermal reprocessing and isotopic exchange after significant decay of ^{26}Al.
2. Stellar nucleosynthetic yields of ^{26}Al are underestimated. In addition, there are uncertainties in the

Table 8. Stable and short-lived nuclei contributions to the presolar cloud by various stellar sources that can produce the canonical value of $^{26}Al/^{27}Al$.

Stellar models		Short-lived nuclides produced along with ^{26}Al	Stable-isotope contributions to the presolar cloud	Inferred isotopic anomalies in CAIs
ONe novae		^{26}Al alone produced	^{15}N and ^{17}O	^{17}O
	T ~0.2 Ma			
CO novae		^{26}Al alone produced	^{13}C, ^{15}N, and ^{17}O	^{17}O
	T ~0.2 Ma			
SNIa		Orders of magnitude high ^{41}Ca, ^{53}Mn, and ^{60}Fe	^{12}C, ^{16}O, and all intermediate-mass isotopes	Isotopes of O, Mg, Si, Ca, Ti
	T ~0.4 Ma			
TP-AGB stars		^{41}Ca and ^{107}Pd produced	$^{12,13}C$, ^{14}N, and ^{17}O	^{17}O [Low magnitude]
1.5 $M_\odot$	T ~0.7 Ma	Low ^{60}Fe		
3 $M_\odot$	T ~0.4 Ma	^{41}Ca, ^{60}Fe, and ^{107}Pd produced	$^{12,13}C$, ^{14}N, ^{17}O, and ^{22}Ne	^{17}O
5 $M_\odot$	T ~0.4 Ma	High ^{41}Ca, ^{60}Fe, and ^{107}Pd	$^{12,13}C$, ^{14}N, ^{17}O & ^{22}Ne	^{17}O
SNII		^{41}Ca, ^{60}Fe, ^{182}Hf , and ^{107}Pd produced	^{12}C to ^{70}Zn isotopes	Isotopes of O, Mg, Si, Ca, Ti
	T ≥ 0.4 Ma	High ^{53}Mn		
	T ~30 yr	^{60}Fe, ^{182}Hf, and ^{107}Pd produced	^{12}C to ^{70}Zn isotopes	Isotopes of O, Mg, Si, Ca, Ti [Reduced magnitude]
	M25			
	O/Ne (Mass cut)	^{41}Ca and ^{60}Fe produced	Mg and Al	Mg isotopes
	T ≥ 0.4 Ma	Low ^{53}Mn		
WR + SNIb/c (binary)		^{41}Ca and ^{60}Fe produced	^{12}C, ^{18}O, and ^{22}Ne	
7–20 $M_\odot$ He stars		High ^{53}Mn		^{18}O
	T ≥ 0.4 Ma			
WR + SNIb/c (Single)		^{41}Ca and ^{60}Fe produced		
40–120 $M_\odot$ stars		High ^{53}Mn	^{12}C to Ca isotopes	Isotopes of O, Mg, Si, Ca, Ti
With wind clumping effects				
	T ≥ 0.4 Ma			
Without wind clumping effects		^{41}Ca and ^{60}Fe produced High ^{53}Mn	^{12}C, ^{22}Ne	Isotopes of O [Low magnitude, along CCAM line]
	T ≥ 0.4 Ma			

Deviations by more than an order of magnitude compared to the empirical estimates of the short-lived nuclei in the early solar system are marked as either high or low.
$^{26}Al/^{27}Al$ ~5×10^{-5} was assumed in the early solar system.

nucleosynthetic yields of various stable nuclei that could result in an overestimate of stable-isotope anomalies.

3. Contrary to the basic assumption, the stellar injection efficiency of the various stable and short-lived nuclei injected into the presolar cloud need not be identical. In addition, the distinct chemical nature of the carriers (dust/gas) of stellar injected stable and short-lived nuclei can differentially influence the temporal and spatial scales involved in the homogenization of freshly injected nuclei in the solar nebula.
4. Stellar nucleosynthesis was not responsible for any significant contribution of ^{26}Al to the early solar system but could have contributed ^{60}Fe.
5. ^{26}Al was produced in cool-bottom processes in low-mass ABG stars. This possibility does not create conflicts in isotopic abundances of stable isotopes, but a quantitative model for such a slow mixing phenomenon has not been presented yet. This deficiency remains clearly the most important drawback of low-mass star models.

Stable-Isotope Systematics of CAIs Devoid of ^{26}Al

CH chondrites are generally considered to be some of the most primitive chondrites. CAIs from these chondrites are mineralogically more refractory than CAIs from other chondrites (MacPherson et al. 1989; Kimura et al. 1993; Weber and Bischoff 1994; Weber et al. 1995; Krot et al. 1999b). None of these CAIs analyzed for Ca, Ti, and Mg isotopes exhibit significant intrinsic isotopic mass fractionation (Kimura et al. 1993; Weber et al. 1995). These CAIs have a simple nebular formation history with no signatures of evaporative losses, low-temperature secondary alterations, or thermal metamorphism. This is also evident from the oxygen isotopic composition of CAIs analyzed from two CH chondrites, Acfer 182 and Patuxent Range (PAT) 91546 (Sahijpal et al. 1999). On the conventional oxygen isotopic plot, these CAIs yielded a slope of 1.02 ± 0.03, with an intercept of -2.2 ± 0.4 (2σ). In addition, the heterogeneity in the oxygen isotopic composition among the various mineral phases within a single CH CAI is small (<10‰), suggesting that these CAIs experienced very little oxygen isotopic exchange following their formation. Based on the mineralogical and isotopic characteristics it seems unlikely that CAIs from CH chondrite underwent significant isotopic homogenization after their formation.

The possibility that the CAIs from CH chondrite were formed late, probably after 3 Ma subsequent to the formation of CAIs with canonical ^{26}Al/^{27}Al seems to be unlikely. This would require elongated nebular time scales for the preservation and/or synthesis of the oxygen isotopic reservoirs representing the observed distribution along the CCAM line of slope ~1. Nonetheless, this possibility cannot be ruled out completely even though the refractory nature of CAIs from CH chondrites along with the absence of secondary alterations suggest that these CAIs were accreted by their parent bodies just after their formation. However, the chronology associated with the various processes involved in the formation of these CAIs and their parent bodies remain unclear. If the CAIs from CH chondrites were formed late in the solar nebula, their pristine oxygen isotopic composition will favor the occurrence of non-mass dependent isotopic fractionation "locally" in the solar nebula (Lyons and Young 2004) rather than in the presolar cloud (Yurimoto and Kuramoto 2004).

In the case of PLAC hibonites from CM chondrites that exhibit large isotopic anomalies in the neutron-rich isotopes of Ca and Ti, the late stage formation of the hibonites seems to be less probable as it would require preservation of the observed stable-isotope anomalies for elongated time scales (Fahey et al. 1987a). Post formation alterations that could have resulted in significant isotopic exchange of most of these refractory phases also seems to be less likely on the basis of the preservation of oxygen (Fahey et al. 1987b; Sahijpal et al. 2000b), ^{48}Ca and ^{50}Ti isotopic anomalies (Fahey et al. 1985, 1987a, 1994; Zinner et al. 1986; Fahey 1988; Ireland et al. 1991; Simon et al. 1998; Sahijpal et al. 2000a). It seems unlikely that PLAC hibonites that could preserve isotopic anomalies in the neutron-rich isotopes of Ca and Ti could not preserve the inferred isotopic anomalies in other isotopes of Ca and Ti.

Uncertainties in Stellar Nucleosynthetic Yields

A plausible explanation for the absence of the inferred stable-isotope anomalies could be due to an underestimated stellar nucleosynthetic yield of ^{26}Al. For example, it is quite likely that ^{26}Al yields of SNII are too low as seems to be supported by the high initial ^{26}Al/^{27}Al (up to 0.6) measured in SiC X grains (Hoppe et al. 2000). Uncertainties in the stellar nucleosynthetic yields could be due to uncertainties in the nuclear reaction rates, stellar mass-loss rates and the stellar physics of mostly non-rotating stellar models. The uncertainties become obvious when comparing nucleosynthetic yields obtained by two different groups for an identical stellar source. For example, the SNII ^{26}Al yields obtained by Rauscher et al (2002) are higher by a factor of 2–4 than the yields obtained by Chieffi and Limongi (2004) (Table 1). In general, there is a discrepancy by a factor of 2–4 in the SNII yields of other short-lived nuclei as well. The uncertainties in the yields would not only have an impact on the role of a SNII as a plausible source of short-lived nuclei to the early solar system but would also influence the SNII contributions to the total galactic inventories of some of the short-lived nuclei, e.g., ^{26}Al and ^{60}Fe. The theoretical ^{60}Fe/^{26}Al ratios obtained from the SNII models by various groups are specifically important in understanding the observed gamma-ray line intensities of ^{26}Al and ^{60}Fe in the Milky Way (Prantzos 2004). The observed value of 0.16 for ^{60}Fe/^{26}Al is significantly smaller than the values recently estimated from SNII yields (Rauscher et al. 2002; Chieffi and Limongi 2004).

This disagreement could imply that Wolf-Rayet stars ($\geq$30 $M_\odot$) or intermediate-mass AGB stars significantly contribute ^{26}Al to the galaxy (Prantzos 2004). This conclusion seems to be supported by the lower estimates of ^{60}Fe/^{26}Al ratios from the Wolf-Rayet stars evolved though SNIb/c, compared to those obtained from the SNII models (Table 1).

In the case of massive Wolf-Rayet stars, incorporation of rotation in the stellar models increases ^{26}Al yields (Knödlseder et al. 2002). Further enhancements in the nucleosynthetic yields of the rotating stellar models have recently been proposed (Palacios et al. 2005). These stellar models not only increase the ^{26}Al production during the WN stage but also result in a relatively small CO-core for the subsequent SNIb/c explosion. The latter would effectively reduce the contributions of stable nuclei from SNIb/c.

Apart from the uncertainties in the stellar yields of ^{26}Al, the nucleosynthetic yields of the various stable nuclei also suffer from uncertainties (Meyer et al. 1999; Nichols et al. 1999). The yields of a specific stellar source are essentially model dependent predictions that could be way off in an absolute sense. As discussed earlier, the uncertainties could be due to the limitations in the stellar physics, the employed nuclear reaction network and the reaction rates. Due to the complexities involved in the determination of nucleosynthetic yields it becomes extremely difficult to quantify the associated uncertainties. However, the systematic errors in the nucleosynthetic yields can be suppressed in some of the cases involving massive stars. This is achieved by mixing the SNII ejecta with the solar system proxy composition rather than the observed cosmic composition (Meyer et al. 1999; Nichols et al. 1999). The solar system proxy composition is obtained from a galactic chemical evolution model based on the SNII yields. In general, this normalization procedure reduces the magnitude of isotopic anomalies for nuclei that are primarily produced by SNIIe. This normalization procedure probably gives better estimates of the isotopic anomalies for the primary isotopes compared to isotopes such as ^{44}Ca, ^{48}Ca, ^{47}Ti, ^{50}Ti, ^{54}Cr, etc., that are either produced in special stellar sources or whose stellar production scenarios are not well defined (Meyer et al. 1999). If this normalization procedure were applied for SNII contributions in the present work, we would anticipate a reduction in the magnitude of stable-isotope anomalies for the isotopes that are primarily produced by SNII. However, in spite of the reduction in the magnitude, as observed by Nichols et al. (1999), the anomalies persist. The predicted anomalies are still resolvable by mass spectroscopy.

To an extent, the normalization procedure to deduce the stable-isotope anomalies can be followed in the case of SNIa. SNIa are considered to be the key contributors of Fe-group nuclei, e.g., ^{48}Ca, ^{50}Ti, and ^{54}Cr, to the galaxy. The galactic chemical evolution model based on the SNIa nucleosynthetic yields (Iwamoto et al. 1999) will also incorporate the associated uncertainties. If we mix the SNIa ejecta with the solar system proxy composition based on this galactic chemical evolution model, the systematic errors in the nucleosynthetic yields of the Fe-group nuclei will be suppressed. This is likely to reduce the magnitude of associated isotopic anomalies. However, an exact treatment of the possible contributions of short-lived and the Fe-group nuclei from SNIa to the presolar cloud would require re-examination of the SNIa nucleosynthetic yields. The yields of the multidimensional hydrodynamical SNIa models (Travaglio et al. 2004) are quite different from the 1-D SNIa models (Iwamoto et al. 1999).

Unlike the SNIa and SNII stellar scenarios, the normalization procedure would not be much effective in the case of intermediate-mass AGB stars, novae and WR + SNIb/c in reducing the magnitude of stable-isotope anomalies. This is essentially due to the fact that most of the stable isotopes relevant to the present work are not exclusively produced by these stellar sources. Since the magnitude of stables isotopic effects are small in the case of low-mass AGB stars, the normalization procedure is not required for these stars.

Injection Efficiency and the Carriers of Stable and Short-Lived Nuclei

When estimating the contributions of stellar nucleosynthetic products to the presolar cloud, it was assumed that nuclei from different stellar zones (e.g., distinct zones of SNII) and of diverse chemical nature were initially mixed and injected with identical injection efficiency η (~0.1). Subsequently, the ejecta were instantaneously homogenized with the collapsing cloud, at least in the CAI forming regions, with a mixing time scale much shorter than the time scale of ~0.1 Ma for the collapse of cloud core following the passage of the shock wave (Boss and Vanhala 2001). These fundamental assumptions regarding the injection and homogenization of ejecta with the cloud core require detailed assessment to understand the implications of the inferred isotopic anomalies.

Numerical simulations of the injection of radially unmixed supernova ejecta into the presolar cloud indicate that nuclei lagging behind those moving along with the shock front are also injected through Rayleigh-Taylor instabilities with identical efficiencies (Boss and Foster 1998). The Rayleigh-Taylor-fingers created by the leading edge of the shock wave can survive for ~0.2 Ma and these fingers can provide a secure passage for the nuclei lagging behind up to 4 pc. Thus, in the case of traditional scenarios that involve injection of short-lived nuclei into the presolar cloud, the basic assumption of an identical injection efficiency of the stable and short-lived nuclei may be appropriate. However, this assumption is not valid in the scenario that involves preferential injection of stellar dust, compared to gas, into the protoplanetary disc (Ouellette and Desch 2004). For example, because oxygen is partitioned between dust and gas phases, the injection of stellar dust alone into the protoplanetary disc

would reduce the injection efficiency of oxygen. This will reduce the magnitude of oxygen isotopic anomalies. However, the preferential injection of dust may not have significant influence on the stable-isotope anomalies associated with the refractory elements.

Even with an identical efficiency of injection, it is quite likely that the injected nuclei, depending upon whether they are brought into the presolar cloud in dust or gas phases, homogenize with the collapsing presolar cloud over different spatial regions with distinct mixing time scales. The chemical environment, specifically, the C/O ratio prevailing in the stellar ejecta, will determine the composition of the condensing dust grains (Ebel and Grossman 2001). The nature of these grains and the physico-chemical environment prevailing in the nebula will influence the homogenization of various stable and short-lived nuclei. Intermediate zones of SNII with C/O < 1 produce oxides and silicates that can bring Ca, Ti, Al, Mg, Si, and O into the presolar cloud. However, in the case of C/O > 1, corresponding to either outer zones of SNII or an evolved AGB stellar envelope, significant condensation of SiC or graphite grains can result in chemical partitioning of O, Si, Ca, Ti, Al, and Mg into dust and gas phases. It would be essential to study the nature of the dust grains that bring in O, Si, Ca, Al, Ti, and Mg to the CAI forming regions of the solar nebula. The extent and the time scale associated with the mixing of these injected dust grains with the accretion disc will depend upon the disc's gravitational torques, thermal convection and turbulent viscosity (Boss 2004). A high-turbulence viscosity disc can mix the injected dust grains with the disc in less than 10^3 yr (Boss 2004). However, a low-turbulence viscosity disc can maintain isotopic heterogeneity over time scales that are comparable to the grain coagulation time scales of ~10^3 yr. This can result in the preservation of isotopic heterogeneity as the dust grains carrying isotopic anomalies are trapped in larger coagulated grains.

Apart from the dynamical conditions prevailing in the disc, the preservation of heterogeneity in ^{26}Al along with any associated heterogeneity in stable nuclei would primarily depend upon whether the heterogeneity in ^{26}Al was temporal or spatial in nature. If the heterogeneity in ^{26}Al was purely temporal in nature, i.e., the CAIs devoid of ^{26}Al formed earlier, it is likely that these CAIs would be isotopically anomalous compared to the CAIs formed after the injection and mixing of stellar ejecta with the disc. As mentioned earlier, in this scenario, subsequent thermal reprocessing of the CAIs devoid of ^{26}Al in the nebula admixed with stellar ejecta can erase the stable-isotope anomalies. Even though this seems to be unlikely in the case of PLAC hibonites and the pristine CAIs from CH chondrites, it cannot be ruled out completely in the former case.

Alternatively, if the formation of CAIs in the ^{26}Al-free and ^{26}Al-rich nebular reservoirs was contemporaneous, it is quite likely that a low-turbulence disc produced the spatial heterogeneity in ^{26}Al over a time scale of ~10^3 yr. If the low-turbulence disc was also experiencing transient heating episodes during the mixing of stellar ejecta with the disc, the repeated vaporization and condensation of dust grains according to their refractory nature could have resulted in homogenization of various injected stable and short-lived nuclei on different time scales. However, it would be difficult to reconcile that ^{26}Al and other refractory elements were homogenized in the disc over different time scales. Hence, the heterogeneity in ^{26}Al would be accompanied by associated heterogeneities in stable nuclei, specifically in the refractory elements. This would result in stable-isotope anomalies as inferred in the present work. Since oxygen is partitioned between dust and gas phases, it is possible that the ^{26}Al-rich and the ^{26}Al-free CAI forming reservoirs acquired identical oxygen isotopic composition quite rapidly.

In general, the absence of the predicted stable-isotope anomalies in both scenarios involving temporal and spatial heterogeneity in ^{26}Al would imply that either the stellar yields of ^{26}Al are underestimated, or ^{26}Al was not produced by stellar nucleosynthesis. However, the case of low-mass AGB stars is an exception to this generality, as it does not predict significant stable-isotope anomalies.

Stellar Contribution of ^{26}Al and Other Short-Lived Nuclei

Even though a wide range of stellar sources can readily produce the canonical value of ^{26}Al/^{27}Al in the early solar system, most of them fall short in explaining the initial abundances of other short-lived nuclei, viz, ^{41}Ca, ^{36}Cl, ^{60}Fe, and ^{53}Mn, in a self-consistent manner (Table 8). If a low-mass 1.5 $M_\odot$TP-AGB star produced ^{26}Al, an additional stellar source would be required to explain the initial ^{60}Fe/^{56}Fe in the early solar system. However, the 3 $M_\odot$ TP-AGB model produces the ^{60}Fe/^{56}Fe ratio within the adopted initial early solar system value if the AGB star has a metallicity slightly lower than solar (Wasserburg et al. 2006). As mentioned earlier, TP-AGB stars within the mass range, 1.5–3 $M_\odot$ are potential producers of the short-lived nuclei ^{26}Al, ^{41}Ca, ^{60}Fe, and ^{107}Pd (Busso et al. 2003). In general, the presence of ^{53}Mn in the early solar system can be explained by steady-state contributions of supernovae to the galaxy prior to the formation of the solar system (Meyer and Clayton 2000; Busso et al. 2003). Hence, a late-stage contribution of ^{53}Mn to the presolar cloud by a stellar source is not essential. In fact, an additional late-stage contribution of ^{53}Mn to the presolar cloud could pose a difficulty for a stellar scenario to be a plausible contributor of short-lived nuclei.

All SNII models with a low-injection mass cut produce higher yields of ^{53}Mn than the models with high injection mass cut. An injection mass cut of ~5 $M_\odot$ for a 25 $M_\odot$ SNII can explain the abundances of all the short-lived nuclei in the early solar system (Meyer et al. 2003, 2004; Meyer 2004). The M25 SNII model with a mass cut at the O/Ne shell,

studied in the present work, results in relatively small isotopic anomalies compared to other SNII models. The magnitude of the stable-isotope anomalies would be further reduced if the stable and short-lived nuclei were injected only into the protoplanetary disc. This model can explain the abundance of all the short-lived nuclei. However, a physical justification for assuming a high mass cut has still to be presented.

If we exclude a significant contribution of ^{26}Al by a massive star, we can still envisage several stellar scenarios (see Table 3, for example) that can produce ^{60}Fe alone and can trigger the gravitational collapse of the presolar cloud. Within these scenarios, the presence of ^{7,10}Be, ^{41}Ca, ^{36}Cl, and ^{26}Al in the early solar system would require irradiation of nebula dust and gas by energetic particles from magnetic flares associated with the protosun and/or its circumstellar accretion disc (Feigelson et al. 2002). However, the irradiation scenario(s) specifically requires ^{3}He-rich impulsive flares (Lee et al. 1998; Gounelle et al. 2001; Shu et al. 2001; Leya et al. 2003) as the gradual flares can produce the required abundance of ^{7,10}Be, ^{41}Ca, ^{36}Cl, and ^{53}Mn but under produce ^{26}Al by a factor of 100 (Goswami et al. 2001). In addition, in order to produce the canonical value of ^{26}Al/^{27}Al in the early solar system, the irradiation scenario(s) would require thorough mixing of the reservoirs of ^{26}Al produced by irradiation (Sahijpal and Soni 2006).

Dynamical Constraints on the Stellar Contribution of ^{26}Al

Massive Stars

In the case of massive stars, the magnitude of the inferred isotopic anomalies is lowest for the scenarios involving stellar injection of short-lived nuclei into the solar protoplanetary disc (Desch and Ouellette 2005). This is due to the extremely short (negligible) free-decay time interval of ~30 yr. However, in the traditional scenarios that involve stellar injection of short-lived nuclei into the presolar cloud (Cameron and Truran 1977), the magnitude of isotopic anomalies increases steadily with the free-decay time interval. Even though it would be difficult to independently impose temporal constraints on the various dynamical processes from the stellar injection of short-lived nuclei into the presolar cloud to the condensation of CAIs in the solar nebula, a lower limit estimate of the free-decay time interval can be made. Prior to its interaction with the presolar cloud, the supernova shock wave would require ~0.1–1 Ma to propagate through the intercloud medium (ICM) depending upon its density. The presolar cloud core can collapse over a time scale of ~0.1 Ma subsequent to the passage of the shock wave (Boss and Vanhala 2001). These two dynamical processes alone would impose a lower limit of ~0.2 Ma on the free-decay time interval. In order to minimize the magnitude of stable-isotope anomalies it would be essential to minimize the free-decay time interval. This would imply propagation of supernova shock waves through a dense ICM (see Tables 2 and 4–6, for example) over a distance <10 pc.

An upper bound on the distance D traveled by the supernova shock wave can be obtained from another argument. In the case of SNII scenarios that can produce the canonical value of ^{26}Al/^{27}Al in the early solar system, the higher estimates of D (>10 pc) would imply a larger presolar cloud core compared to that used in the numerical simulations of triggered star formation (Vanhala and Boss 2002). A larger cloud core would imply a much smaller central density of the ~1 $M_{\odot}$ presolar cloud core, e.g., S25 SNII at a distance of 40 pc (Table 2) would imply an average density $\leq 7 \times 10^{-25}$ gm cm^{-3} of the presolar cloud, compared to the central density of $\sim 6 \times 10^{-19}$ gm cm^{-3} used in the numerical simulations (Vanhala and Boss 2002). If we use 45 km s^{-1}, instead of 10 km s^{-1}, as the final velocity of the SNII shock wave prior to its interaction with the presolar cloud, the resulting density will increase only by a factor of four. It may be dynamically implausible to trigger the collapse of this low-density molecular cloud. Within this scenario, the SNII would just contribute short-lived nuclei to the presolar cloud, whereas the gravitational collapse of the cloud would take place probably by ambipolar diffusion of magnetic field lines. This imposes a stringent constraint on the distance of the supernova contributing ^{26}Al to be <10 pc, probably, a couple of parsecs, in case the supernova also triggered the gravitational collapse of the presolar cloud. In contrast, the relatively "distant" (≥10 pc) supernova scenarios (Table 3) that exclude a significant contribution of ^{26}Al but nonetheless contribute ^{60}Fe to the presolar cloud, imply a higher central density of the presolar cloud for a free-decay time interval of ~2 Ma. This "distant" supernova could have triggered the gravitational collapse of the presolar cloud core.

There are few astronomical observations of supernova-triggered star formation, also by supernovae at distances >10 pc from dense molecular clouds (Preibisch and Zinnecker 1999; Kothes et al. 2001). A supernova explosion can trigger a burst of star formation of low-mass and massive stars within a molecular cloud. These regions of active star formation are generally found within OB associations where stellar winds and supernova explosions not only initially trigger star formation but also are also responsible for the final disruption of the molecular cloud. The inferred distances of <10 pc for the various supernova scenarios that can significantly contribute ^{26}Al to the presolar cloud fall short of the astronomical observations. A triggered collapse of the presolar cloud by a "near-by" supernova along with a significant contribution of ^{26}Al would require fine-tuning of the various dynamical parameters. This would include the size (or density) of the presolar cloud core, the injection efficiency η, the free-decay time interval and the density profile of the ICM through which the supernova shock wave propagates. This would also necessitate an early supernova-triggered event during the lifetime of the parent molecular cloud prior to its disruption by stellar winds and supernova explosions. The probability that the solar system formed in such an environment by the gravitational collapse triggered

by a 25 $M_\odot$ supernova has been estimated to be ~0.008 (Adams and Laughlin 2001). The probability is reduced to ~0.0025, in case a 60 $M_\odot$ massive star triggered the gravitational collapse of the presolar cloud. Even though the WR + SNIb/c scenarios involving massive stars, e.g., a 60 $M_\odot$ star, result in relatively smaller stable-isotope anomalies than SNII models (Tables 2, 5, and 6), the former scenario is less probable essentially due to the stellar initial mass function.

Among all the proposed massive stellar scenarios contributing ^{26}Al, the injection of short-lived nuclei into the protoplanetary disk seems to be more viable (Desch and Ouellette 2005). Apart from the smallest stable-isotope anomalies (Table 2), this scenario seems to be well supported by the astronomical observations of numerous protoplanetary disks around massive stars in OB associations, e.g., the Orion nebula. These protoplanatery discs are formed because of the triggered collapse of dense molecular cloud cores by the shock waves associated with the ionization front and stellar winds of the massive stars. Depending upon the mass of the most massive, and hence, the most rapidly evolving, star, the protoplanetary disc could later be contaminated by short-lived nuclei either from a WR + SNIb/c (≥30 $M_\odot$) or a SNII (~25 $M_\odot$). The former scenario would be more relevant in the case of the θ^1Ori C (40 $M_\odot$) star in the Orion nebula.

AGB Stars, Nova, and SNIa

Among the various proposed stellar sources of short-lived nuclei, AGB stars, nova and SNIa are less likely to be associated with molecular clouds compared to massive stars that evolve rapidly. The probability of a close encounter of a mass-losing AGB star with a molecular cloud has been estimated to be one in 1 Ma. At the time of formation of the solar system, this could have been a little higher (Busso et al. 1999). As AGB winds have a typical velocity of ~10 km s^{-1}, these winds are unlikely to trigger the gravitational collapse of the presolar cloud. The maximum distance covered by AGB winds before slowing to a velocity of ~1 km s^{-1} is ~3 pc (Table 7). AGB winds may be dispersed in the random motions of the ICM before traveling such distances. Even if an AGB star contaminates a molecular cloud with short-lived nuclei, the gravitational collapse of the molecular cloud would probably still occur by ambipolar diffusion of magnetic field lines. The contribution of ^{26}Al from an AGB star would impose a temporal constraint of ≤1 Ma in this scenario.

The case of a classical nova that contributed ^{26}Al to the presolar cloud and triggered its gravitational collapse seems to be unlikely. As mentioned earlier, invariably most of the classical nova models contaminate only a fraction of the ~1 $M_\odot$ presolar cloud to produce the canonical value of ^{26}Al/^{27}Al in that particular fraction. Classical novae generally have extremely small mass ejections of (0.5–7) × 10^{-5} $M_\odot$ (José and Hernanz 1998). For a typical ejection velocity of 2 × 10^3 km s^{-1}, the shock wave associated with a nova will slow to a velocity of ~10 km s^{-1} in 10^4 yr after covering a distance of 0.3 pc through a ICM of a constant density of 10^{-23} gm cm^{-3}. In the extreme case, the shock wave can travel ~0.5 pc to end up with a final velocity of ~1 km s^{-1}. However, it is more likely to be dispersed by the ICM before covering this distance. In spite of a high galactic rate of nova occurrences (~30 events yr^{-1}), it seems to be unlikely that a dense molecular cloud core could be associated with a nova within 0.5 pc. A typical molecular cloud with a lifetime of few tens of millions of years is unlikely to be associated with a white dwarf accreting matter from its binary.

A close encounter of a SNIa with the presolar cloud also seems to be implausible. This scenario is almost identical to the one involving a close encounter of a nova with the presolar cloud except for the higher mass ejected by SNIa that can contaminate a larger region of the ICM. Even though there is no observational evidence of any SNIa encounter with a molecular cloud core, significant contribution of ^{60}Fe to the presolar cloud by a SNIa cannot be ruled out completely (Table 4).

CONCLUSIONS

In order to produce the canonical value of ^{26}Al/^{27}Al in the early solar system most of the proposed stellar sources yield significant stable-isotope anomalies in the CAIs formed in the ^{26}Al-free nebular reservoirs compared to those formed in the ^{26}Al-rich reservoir. None of these isotopic anomalies have been observed. The magnitude of the stable-isotope anomalies is minimal in the case of 1.5 $M_\odot$ TP-AGB star and the stellar scenarios involving injection of short-lived nuclei into the protoplanetary disc by massive stars. The latter could involve either a SNII with a high injection mass-cut or a Wolf-Rayet star evolved to SNIb/c but at the present level of uncertainties only order of magnitude estimates are possible. The predicted stable-isotope anomalies would impose stringent constraints on the source(s) of short-lived nuclei and/or the formation of CAIs from different chondrites. However, several aspects associated with the inferred stable-isotope anomalies need to be addressed. These include uncertainties in the stellar nucleosynthetic yields, the injection efficiency of the various nuclei and the dynamics involved in the homogenization of injected dust and gas with the CAI-forming nebular reservoirs.

Distinct from the stellar scenarios contributing ^{26}Al to the early solar system, several alternative scenarios can be postulated that would produce none of the stable-isotope anomalies. A distant (≥10 pc) supernova could have contributed ^{60}Fe to the presolar cloud and triggered its gravitational collapse. However, this scenario would require irradiation production of ^{26}Al in the early solar system by energetic particles from impulsive flares.

Acknowledgments–We are extremely grateful to Drs. G. Meynet and A. I. Karakas for providing nucleosynthesis data of Wolf-Rayet and AGB stars, respectively. We are also

extremely grateful to Drs. M. Busso, P. Hoppe, E. K. Zinner and an anonymous reviewer for their reviews and valuable comments that helped in the general improvement of this manuscript. We are thankful for their suggestions to incorporate the recent stellar nucleosynthetic yields and the dynamical aspects associated with the stellar injection of short-lived nuclei. We sincerely appreciate the comments made by the associate editor and the reviewers to improve the language of this manuscript. This work was supported by the PLANEX grant of Indian Space Research Organization (ISRO). We are thankful to the associateship program of the Inter-University Centre for Astronomy and Astrophysics (IUCAA), Pune.

Editorial Handling—Dr. Ernst Zinner

REFERENCES

Adams F. C. and Laughlin G. 2001. Constraints on the birth aggregate of the solar system. *Icarus* 150:151–162.

Anders E. and Grevesse N. 1989. Abundances of the elements. *Geochimica et Cosmochimica Acta* 53:197–214.

Birck J. L., Rotaru M., and Allègre C. J. 1999. ^{53}Mn-^{53}Cr evolution of the early solar system. *Geochimica et Cosmochimica Acta* 63: 4111–4117.

Boss A. P. 2004. Evolution of the solar nebula. VI. Mixing and transport of isotopic heterogeneity. *The Astrophysical Journal* 616:1265–1277.

Boss A. P. and Foster P. N. 1998. Injection of short-lived isotopes into the presolar cloud. *The Astrophysical Journal* 494:103–106.

Boss A. P. and Vanhala H. A. T. 2001. Injection of newly synthesized elements into the protosolar cloud. *Philosophical Transactions of the Royal Society of London A* 359:2005–2017.

Busso M., Gallino R., and Wasserburg G. J. 1999. Nucleosynthesis in asymptotic giant branch stars: Relevance for galactic enrichment and solar system formation. *Annual Review of Astronomy and Astrophysics* 37:239–309.

Busso M., Gallino R., and Wasserburg G. J. 2003. Short-lived nuclei in the early solar system: A low-mass stellar source? *Publications of the Astronomical Society of Australia* 20:356–370.

Cameron A. G. W. 1993. Nucleosynthesis and star formation. In *Protostars and planets III*, edited by Levy E. H. and Lunine J. I. Tucson, Arizona: The University of Arizona Press. pp. 47–73.

Cameron A. G. W. 2003. Some nucleosynthesis effects associated with r-process jets. *The Astrophysical Journal* 587:327–340.

Cameron A. G. W. and Truran J. W. 1977. The supernova trigger for formation of the solar system. *Icarus* 30:447–461.

Cameron A. G. W., Höflich P., Myers P. C., and Clayton D. D. 1995. Massive supernova, Orion gamma rays, and the formation of the solar system. *The Astrophysical Journal* 447:53–57.

Cameron A. G. W., Vanhala H. A. T., and Höflich P. 1997. Some aspects of triggered star formation. In *Astrophysical implications of the laboratory study of pre-solar materials*, edited by Bernatowicz T. J. and Zinner E. New York: American Institute of Physics. pp. 665–693.

Cerviño M., Knödlseder J., Schaerer D., von Ballmoos P., and Meynet G. 2000. Gamma-ray line emission from OB associations and young open clusters. I. Evolutionary synthesis models. *Astronomy and Astrophysics* 363:970–983.

Chaussidon M., Robert F., and McKeegan K. D. 2004. Li and B isotopic variations in Allende type B1 CAI 3529-41: Traces of incorporation of short-lived ^{7}Be and ^{10}Be (abstract #1568). 35th Lunar and Planetary Science Conference. CD-ROM.

Chieffi A. and Limongi M. 2004. Explosive yields of massive stars from Z = 0 to Z = Z. *The Astrophysical Journal* 608:405–410.

Clayton R. N. 1993. Oxygen isotopes in meteorites. *Annual Review of Earth and Planetary Sciences* 21:115–149.

Clayton R. N. 2002. Photochemical self-shielding in the solar nebula (abstract #1326). 33rd Lunar and Planetary Science Conference. CD-ROM.

Desch S. J. and Ouellette N. 2005. The meaning of iron-60: A nearby supernova injected short-lived radionuclides into our protoplanetary disk (abstract #1327). 36th Lunar and Planetary Science Conference. CD-ROM.

Ebel D. S. and Grossman L. 2001. Condensation from supernova gas made of free atoms. *Geochimica et Cosmochimica Acta* 65:469–477.

Fahey A. J. 1988. Ion microprobe measurements of Mg, Ca, Ti, and Fe isotopic ratios and trace element abundances in hibonite-bearing inclusions from primitive meteorites. Ph.D. thesis, Washington University, Saint Louis, Missouri, USA.

Fahey A. J., Goswami J. N., McKeegan K. D., and Zinner E. 1985. Evidence for extreme ^{50}Ti enrichments in primitive meteorites. *The Astrophysical Journal* 296:17–20.

Fahey A. J., Goswami J. N., McKeegan K. D., and Zinner E. K. 1987a. ^{26}Al, ^{244}Pu, ^{50}Ti, REE, and trace element abundances in hibonite grains from CM and CV meteorites. *Geochimica et Cosmochimica Acta* 51:329–350.

Fahey A. J., Goswami J. N., McKeegan K. D., and Zinner E. K. 1987b. ^{16}O excesses in Murchison and Murray hibonites: A case against a late supernova injection origin of isotopic anomalies in O, Mg, Ca, and Ti. *The Astrophysical Journal* 323:91–95.

Fahey A. J., Zinner E. K., Kurat G., and Kracher A. 1994. Hibonite-hercynite inclusion HH-1 from the Lancé (CO3) meteorite: The history of an ultrarefractory CAI. *Geochimica et Cosmochimica Acta* 58:4779–4793.

Feigelson E. D., Garmire G. P., and Pravdo S. H. 2002. Magnetic flaring in the pre-main-sequence sun and implications for the early solar system. *The Astrophysical Journal* 572:335–349.

Forestini M. and Charbonnel C. 1997. Nucleosynthesis of light elements inside thermally pulsing AGB stars. I. The case of intermediate-mass stars. *Astronomy and Astrophysics* 123:241–272.

Goswami J. N. and Vanhalla H. A. T. 2000. Extinct radionuclei and the origin of the solar system. In *Protostars and Planets IV,* edited by Mannings V. Boss A. P., and Russell S. S. Tucson, Arizona: The University of Arizona Press. pp. 963–994.

Goswami J. N., Marhas K. K., and Sahijpal S. 2001. Did solar energetic particles produce the short-lived nuclides present in the early solar system? *The Astrophysical Journal* 549:1151–1159.

Gounelle M., Shu F. H., Shang H., Glassgold A. E., Rehm K. E., and Lee T. 2001. Extinct radioactivities and protosolar cosmic rays: Self-shielding and light elements. *The Astrophysical Journal* 548:1051–1070.

Hoppe P., Strebel R., Eberhardt P., Amari S., and Lewis R. S. 2000. Isotopic properties of silicon carbide X grains from Murchison meteorite in the size range 0.5–1.5 μm. *Meteoritics & Planetary Science* 35:1157–1176.

Ireland T. R. 1988. Correlated morphological, chemical, and isotopic characteristics of hibonites from the Murchison carbonaceous chondrite. *Geochimica et Cosmochimica Acta* 52:2827–2839.

Ireland T. R. 1990. Pre-solar isotopic and chemical signatures in hibonite-bearing refractory inclusions from the Murchison carbonaceous chondrite. *Geochimica et Cosmochimica Acta* 54: 3219–3237.

Ireland T. R., Fahey A. J., and Zinner E. K. 1991. Hibonite-bearing microspherules: A new type of refractory inclusions with large isotopic anomalies. *Geochimica et Cosmochimica Acta* 55:367–379.

Iwamoto K., Brachwitz F., Nomoto K., Kishimoto N., Umeda H., Hix W. R., and Thielemann F.-K. 1999. Nucleosynthesis in Chandrasekhar mass models for Ia supernovae and constraints on progenitor systems and burning-front propagation. *The Astrophysical Journal* 125:439–462.

José J. and Hernanz M. 1998. Nucleosynthesis in classical novae: CO versus ONe white dwarfs. *The Astrophysical Journal* 494:680–690.

Karakas A. I. 2003. Asymptotic giant branch stars: Their influence on binary systems and the interstellar medium. Ph.D. thesis, Monash University, Clayton, Australia.

Karakas A. I. and Lattanzio J. C. 2003. Production of aluminium and the heavy magnesium isotopes in asymptotic giant branch stars. *Publications of the Astronomical Society of Australia* 20:279–293.

Kelly W. R. and Wasserburg G. J. 1978. Evidence for the existence of Pd-107 in the early solar system. *Geophysical Research Letters* 5:1079–1082.

Kimura M., El Goresy A., Palme H., and Zinner E. 1993. CAIs in the unique chondrites ALH 85085: Petrology, chemistry, and isotopic compositions. *Geochimica et Cosmochimica Acta* 57: 2329–2359.

Kleine T., Münker C., Mezger K., and Palme H. 2002. Rapid accretion and early core formation on asteroids and the terrestrial planets from Hf-W chronometry. *Nature* 418:952–955.

Knüdlseder J., Cerviño M., Le Duigou J.-M., Meynet G., Schaerer D., and von Ballmoos P. 2002. Gamma-ray line emission from OB associations and young open clusters. II. The Cygnus region. *Astronomy and Astrophysics* 390:945–960.

Kothes R., Uyaniker B., and Pineault S. 2001. The supernova remnant G106.3 + 2.7 and its pulsar-wind nebula: Relics of triggered star formation in a complex environment. *The Astrophysical Journal* 560:236–243.

Krot A. N., Sahijpal S., McKeegan K. D., Weber D., Greshake A., Ulyanov A. A., Hutcheon I. D., and Keil K. 1999a. Mineralogy, aluminum-magnesium, and oxygen-isotopic studies of the relic calcium-aluminum-rich inclusions in chondrules. *Meteoritics & Planetary Science* 34:A68–A69.

Krot A. N., Sahijpal S., McKeegan K. D., Weber D., Ulyanov A. A., Petaev M. I., Meiborn A., and Keil K. 1999b. Unique mineralogy and isotopic signatures of CAIs from the CH chondrite Acfer182 (abstract). *Meteoritics & Planetary Science* 34:A69–A70.

Lee T. 1988. Implications of isotopic anomalies for nucleosynthesis. In *Meteorites and the early solar system*, edited by Kerridge J. F. and Matthews M. S. Tucson, Arizona: The University of Arizona Press. pp. 1063–1089.

Lee T., Russell W. A., and Waserburg G. J. 1979. Calcium isotopic anomalies and the lack of aluminum-26 in an unusual Allende inclusion. *The Astrophysical Journal* 228:93–98.

Lee T., Shu F. H., Shang H., and Rehm K. E. 1998. Protostellar cosmic rays and extinct radioactivities in meteorites. *The Astrophysical Journal* 506:898–912.

Leya I., Halliday A. N., and Wieler R. 2003. The predictable collateral consequences of nucleosynthesis by spallation reactions in the early solar system. *The Astrophysical Journal* 594:605–616.

Limongi M., Straniero O., and Chieffi A. 2000. Massive stars in the range 13–25 $M_{\odot}$: Evolution and nucleosynthesis. II. The solar metallicity models. *The Astrophysical Journal* 129:625–664.

Lin Y., Guan Y., Leshin L. A., Ouyang Z., and Wang D. 2004. Evidence for live ^{36}Cl in CAIs from the Ningqiang carbonaceous chondrites (abstract #2084). 35th Lunar and Planetary Science Conference. CD-ROM.

Lugmair G. W. and Shukolyukov A. 1998. Early solar system time scales according to ^{53}Mn-^{53}Cr systematics. *Geochimica et Cosmochimica Acta* 62:2863–2886.

Lyons J. R. 2005. The ^{17}O/^{18}O ratio associated with CO photodissociation in the solar nebula (abstract #2037). 36th Lunar and Planetary Science Conference. CD-ROM.

Lyons J. R. and Young E. D. 2004. Evolution of oxygen isotopes in the solar nebula (abstract #1970). 35th Lunar and Planetary Science Conference. CD-ROM.

MacPherson G. J., Davis A. M., and Grossman J. N. 1989. Refractory inclusions in the unique chondrite ALH 85085 (abstract). *Meteoritics* 24:297.

MacPherson G. J., Davis A. M., and Zinner E. K. 1995. The distribution of aluminum-26 in the early solar system—A reappraisal. *Meteoritics* 30:365–386.

Makide K., Kobayashi S., and Yurimoto H. 2004. Aluminium-26 and oxygen isotopic distributions of CAIs from Acfer 214 CH chondrite (abstract #9076). Workshop on Chondrites and the Protoplanetary Disk. CD-ROM.

McKeegan K. D., Chaussidon M., and Robert F. 2000. Incorporation of short-lived ^{10}Be in a calcium-aluminum-rich inclusion from the Allende meteorite. *Science* 289:1334–1337.

Meyer B. S. 2004. Nucleosynthesis of short-lived radioactivities in massive stars (abstract # 9089). Workshop on Chondrites and the Protoplanetary Disk. CD-ROM.

Meyer B. S. and Clayton D. D. 2000. Short-lived radioactivities and the birth of the sun. *Space Science Reviews* 99:133–152.

Meyer B. S., Weaver T. A., and Woosley S. E. 1995. Isotope source table for a 25 $M_{\odot}$ supernova. *Meteoritics* 30:325–334.

Meyer B. S., Nichols R. H., Podosek F. A., and Jennings C. L. 1999. Subtleties in computing anomalies from late nucleosynthetic additions to the protosolar nebula (abstract #1904). 30th Lunar and Planetary Science Conference. CD-ROM.

Meyer B. S., Clayton D. D., The L.-S., and Eid M. F. El. 2003. Injection of ^{182}Hf into the early solar nebula (abstract #2074). 34th Lunar and Planetary Science Conference. CD-ROM.

Meyer B. S., The L.-S., Clayton D. D., and Eid M. F. El. 2004. Helium-shell nucleosynthesis and extinct radionuclei (abstract #1908). 35th Lunar and Planetary Science Conference. CD-ROM.

Meynet G., Arnould M., Prantzos N., and Paulus G. 1997. Contribution of Wolf-Rayet stars to the synthesis of ^{26}Al. I. The gamma-ray connection. *Astronomy and Astrophysics* 320:460–468.

Meynet G., Arnould M., Paulus G., and Maeder A. 2001. Wolf-Rayet star nucleosynthesis and the isotopic composition of the galactic cosmic rays. *Space Science Reviews* 99:73–84.

Mostefaoui S., Lugmair G. W., Hoppe P., and El Goresy A. 2003. Evidence for live iron-60 in Semarkona and Chervony Kut: A nanoSIMS study (abstract #1585). 34th Lunar and Planetary Science Conference. CD-ROM.

Mostefaoui S., Lugmair G. W., Hoppe P., and El Goresy A. 2004. Evidence for live ^{60}Fe in meteorites. *New Astronomy Review* 48: 155–159.

Mostefaoui S., Lugmair G. W., and Hoppe P. 2005. ^{60}Fe: A heat source for planetary differentiation from a nearby supernova explosion. *The Astrophysical Journal* 625:271–277.

Nakamura T., Mazzall P. A., Nomoto K., and Iwamoto K. 2001a. Light curve and spectral models for the hypernova SN 1998bw associated with GRB 980425. *The Astrophysical Journal* 550: 991–999.

Nakamura T., Umeda H., Iwamoto K., Nomoto K., Hashimoto M.-A., Hix W. R., and Thielemann F.-K. 2001b. Explosive nucleosynthesis in hypernovae. *The Astrophysical Journal* 555: 880–899.

Nichols R. H., Jr., Podosek F. A., Meyer B. S., and Jennings C. L. 1999. Collateral consequences of the inhomogenous distribution of short-lived radionuclei in the solar nebula. *Meteoritics & Planetary Sciences* 34:869–884.

Nollett K. M., Busso M., and Wasserburg G. J. 2003. Cool bottom processes on the thermally pulsing asymptotic giant branch and the isotopic composition of circumstellar dust grains. *The Astrophysical Journal* 582:1036–1058.

Nomoto K., Mazzall P. A., Nakamura T., Iwamoto K., Maeda K., Suzuki T., Turatto M., Danziger I. J., and Patat F. 2001a. The properties of hypernovae: SNe Ic 1998bw, 1997ef, and SNIIn 1997cy. In *Supernovae and gamma-ray bursts: The greatest explosions since the Big Bang*, edited by Livio M., Panagia N., and Sahu K. New York: Cambridge University Press. pp. 144–170.

Nomoto K., Maeda K., Mochizuki Y., Kumagai S., Umeda H., Nakamura T., and Tanihata I. 2001b. Gamma-ray signatures of supernovae and hypernovae. In *Gamma 2001: Gamma-ray astrophysics*, edited by Ritz S., Gehrels N., and Shrader C. R. New York: American Institute of Physics. pp. 487–497.

Olive K. A. and Schramm D. N. 1982. OB associations and the non-universality of the cosmic abundances: Implications for cosmic rays and meteorites. *The Astrophysical Journal* 257:276–282.

Ouellette N. and Desch S. J. 2004. Late injection of radionuclides into solar nebula analogs in Orion (abstract #2116). 35th Lunar and Planetary Science Conference. CD-ROM.

Padmanabhan T. 2001. *Theoretical astrophysics: Stars and stellar systems vol. II*, 1st ed. Cambridge: Cambridge University Press. 575 p.

Palacios A., Meynet G., Vuissoz C., Knödlsedöer J., Schaerer D., Cerviño M., and Mowlavi N. 2005. New estimates of the contribution of Wolf-Rayet stellar winds to the galactic ^{26}Al. *Astronomy and Astrophysics* 429:613–624.

Podosek F. A. and Nichols R. H., Jr. 1997. Short-lived radionuclei in the solar nebula. In *Astrophysical implications of the laboratory study of pre-solar materials*, edited by Bernatowicz T. J. and Zinner E. New York: American Institute of Physics. pp. 617–647.

Prantzos N. 2004. Radioactive ^{26}Al and ^{60}Fe in the Milky Way: Implications of the RHESSI detection of ^{60}Fe. *Astronomy and Astrophysics* 420:1033–1037.

Preibisch T. and Zinnecker H. 1999. The history of low-mass star formation in the upper Scorpius OB association. *The Astrophysical Journal* 117:2381–2397.

Rauscher T., Heger A., Hoffman R. D., and Woosley S. E. 2002. Nucleosynthesis in massive stars with improved nuclear and stellar physics. *The Astrophysical Journal* 576:323–348.

Sahijpal S. 2002a. Stable and radiogenic isotopic constraints on the role of core-collapse supernova as a source of short-lived nuclei (abstract #1095). 33rd Lunar and Planetary Science Conference. CD-ROM.

Sahijpal S. 2002b. Stellar nucleosynthetic contribution of ^{26}Al to the early solar system: Stable-isotope constraints (abstract). *Meteoritics & Planetary Science* 37:A124.

Sahijpal S. and Goswami J. N. 1998. Refractory phases in primitive meteorites devoid of ^{26}Al and ^{41}Ca: Representative samples of first solar system solids? *The Astrophysical Journal* 509:137–140.

Sahijpal S. and Soni P. 2003. Contributions of short-lived nuclei by Wolf-Rayet stars and supernovae I b/c to the early solar system (abstract #1087). 34th Lunar and Planetary Science Conference. CD-ROM.

Sahijpal S. and Soni P. 2004. Production of short-lived nuclides by magnetic flaring in the early solar system (abstract #5056). *Meteoritics & Planetary Science*. 39:A94.

Sahijpal S. and Soni P. Forthcoming. Numerical simulations of production of extinct short-lived nuclei by magnetic flaring in the early solar system. *Meteoritics & Planetary Science*.

Sahijpal S., Goswami J. N., Davis A. M., Grossman L., and Lewis R. S. 1998. A stellar origin for the short-lived nuclei in the early solar system. *Nature* 391:559–561.

Sahijpal S., McKeegan K. D., Krot A. N., Weber D., and Ulyanov A. A. 1999. Oxygen isotopic compositions of CAIs from the CH chondrites, Acfer 182 and PAT 91546 (abstract). *Meteoritics & Planetary Science* 34:A101.

Sahijpal S., Goswami J. N., and Davis A. M. 2000a. K, Mg, Ti, and Ca isotopic compositions and refractory trace element abundances in hibonites from CM and CV meteorites: Implications for early solar system processes. *Geochimica et Cosmochimica Acta* 64:1989–2005.

Sahijpal S., McKeegan K. D., Goswami J. N., and Davis A. M. 2000b. Oxygen isotopic compositions of Murchison hibonites with wide-ranging radiogenic and neutron-rich stable-isotope anomalies (abstract #1502). 31st Lunar and Planetary Science Conference. CD-ROM.

Schramm D. N. and Olive K. A. 1982. Chemical evolution of OB associations. In *Symposium on the Orion nebula to honor Henry Draper*, edited by Glassgold A. E., Huggins P. J., and Schucking E. L. New York: New York Academy of Sciences. pp. 236–242.

Scott E. R. D. and Krot A. N. 2001. Oxygen isotopic compositions and origins of calcium-aluminum-rich inclusions and chondrules. *Meteoritics & Planetary Sciences* 36:1307–1319.

Shu F. H., Shang H., Gounelle M., Glassgold A. E., and Lee T. 2001. The origin of chondrules and refractory inclusions in chondritic meteorites. *The Astrophysical Journal* 548:1029–1050.

Simon S. B., Davis A. M., Grossman L., and Zinner E. K. 1998. Origin of hibonite-pyroxene spherules found in carbonaceous chondrites. *Meteoritics & Planetary Science* 33:411–424.

Srinivasan G., Ulyanov A. A., and Goswami J. N. 1994. Ca-41 in the early solar system. *The Astrophysical Journal* 431:67–70.

Tachibana S. and Huss G. R. 2003. The initial abundance of ^{60}Fe in the solar system. *The Astrophysical Journal* 588:41–44.

Thielemann F.-K., Nomoto K., and Hashimoto M.-A. 1996. Core-collapse supernovae and their ejecta. *The Astrophysical Journal* 460:408–436.

Travaglio C., Hillebrandt W., Reinecke M., and Thielemann F.-K. 2004. Nucleosynthesis in multi-dimensional SN1a explosions. *Astronomy and Astrophysics* 425:1029–1040.

Vanhala H. A. T. and Boss A. P. 2002. Injection of radioactivities into the forming solar system. *The Astrophysical Journal* 575:1144–1150.

Virag A., Zinner E., Amari S., and Anders E. 1991. An ion microprobe study of corundum in the Murchison meteorite: Implications for Al and O in the early solar system. *Geochimica et Cosmochimica Acta* 55:2045–2062.

Wasserburg G. J., Gallino R., and Busso M. 1998. A test of supernova trigger hypothesis with ^{60}Fe and ^{26}Al. *The Astrophysical Journal* 500:189–193.

Wasserburg G. J., Busso M., Gallino R., and Nollett K. M. Forthcoming. Short-lived nuclei in the early solar system: Possible AGB sources. *Nuclear Physics*.

Weber D. and Bischoff A. 1994. The occurence of grossite ($CaAl_4O_7$) in chondrites. *Geochimica et Cosmochimica Acta* 58:3855–3877.

Weber D., Zinner E., and Bischoff A. 1995. Trace element abundances and magnesium, calcium, and titanium isotopic composition of grossite-containing inclusions from the carbonaceous chondrite Acfer 182. *Geochimica et Cosmochimica Acta* 59:803–823.

Wiens R. C., Huss G. R., and Burnett D. S. 1999. The solar oxygen-

isotopic composition: Predictions and implications for solar nebula processes. *Meteoritics & Planetary Science* 34:99–107.

Woosley S. E. and Weaver T. A. 1995. The evolution and explosion of massive stars. II. Explosive hydrodynamics and nucleosynthesis. *The Astrophysical Journal* 101:181–235.

Woosley S. E., Langer N., and Weaver T. A. 1993. The evolution of massive stars including mass loss: Presupernova models and explosion. *The Astrophysical Journal* 411:823–839.

Woosley S. E., Langer N., and Weaver T. A. 1995. The presupernova evolution and explosion of helium stars that experience mass loss. *The Astrophysical Journal* 448:315–338.

Woosley S. E., Heger A., and Weaver T. A. 2002. The evolution and explosion of massive stars. *Reviews of Modern Physics* 74:1015–1071.

Yurimoto H. and Kuramoto K. 2004. Molecular cloud origin for the oxygen isotopic heterogeneity in the solar system. *Science* 305: 1763–1766.

Zinner E. K., Fahey A. J., Goswami J. N., Ireland T. R., and McKeegan K. D. 1986. Large Ca-48 anomalies are associated with Ti-50 anomalies in Murchison and Murray hibonites. *The Astrophysical Journal* 311:103–107.